

Evolution of Hyperphalangy and Digit Reduction in the Cetacean Manus

LISA NOELLE COOPER,^{1*} ANNALISA BERTA,² SUSAN D. DAWSON,³
AND JOY S. REIDENBERG⁴

¹Anatomy Department, Northeastern Ohio Universities College of Medicine, Rootstown,
and School of Biomedical Sciences, Kent State University, Kent, Ohio

²Department of Biology, San Diego State University, San Diego, California

³Department of Biomedical Sciences, Atlantic Veterinary College, Charlottetown,
Prince Edward Island, Canada

⁴Center for Anatomy and Functional Morphology, Mount Sinai School of Medicine,
New York, New York

ABSTRACT

Cetaceans (whales, dolphins, and porpoises) have a soft tissue flipper that encases most of the forelimb, and elongated digits with an increased number of phalanges (hyperphalangy). In addition, some cetaceans exhibit a reduction in digit number. Although toothed cetaceans (odontocetes) are pentadactylous, most baleen whales (mysticetes) are tetradactylous and also lack a metacarpal. This study conducts a survey of cetacean metacarpal and phalangeal morphologies, traces the evolution of hyperphalangy in a phylogenetic context, optimizes characters onto previously published cetacean phylogenies, and tests various digit loss hypotheses. Dissections were performed on 16 cetacean flippers representing 10 species (8 mysticetes, 2 odontocetes). Phalangeal count data were derived from forelimb radiographs (36 odontocetes, 5 mysticetes), osteological specimens of articulated forelimbs (8 mysticetes), and were supplemented with published counts. Modal phalangeal counts were coded as ordered and unpolarized characters and optimized onto two known cetacean phylogenies. Results indicate that digital ray I is reduced in many cetaceans (except *Globicephala*) and all elements of digital ray I were lost in tetradactylous mysticetes. Fossil evidence indicates this ray may have been lost approximately 14 Ma. Most odontocetes also reduce the number of phalangeal elements in digit V, while mysticetes typically retain the plesiomorphic condition of three phalanges. Results from modal phalangeal counts show the greatest degree of hyperphalangy in digits II and III in odontocetes and digits III and IV in mysticetes. Fossil evidence indicates cetacean hyperphalangy evolved by at least 7–8 Ma. Digit loss and digit positioning may underlie disparate flipper shapes, with narrow, elongate flippers facilitating fast swimming and broad flippers aiding slow turns. Hyperphalangy may help distribute leading edge forces, and multiple interphalangeal joints may smooth leading edge flipper contour. Anat Rec, 290:654–672, 2007. © 2007 Wiley-Liss, Inc.

Key words: forelimb; whale; cetacean; digit loss; hyperphalangy; tetradactyly; flipper

Grant sponsor: NSF, Grant number: DEB 0212248; NOAA, Grant number: NA03NMF4390402.

*Correspondence to: Lisa N. Cooper, Anatomy Department, Northeastern Ohio Universities College of Medicine, 4209 State Route 44, Rootstown, OH 44272-0095.
E-mail: lisa1225cooper@yahoo.com

Received 2 March 2007; Accepted 6 March 2007

DOI 10.1002/ar.20532

Published online in Wiley InterScience (www.interscience.wiley.com).

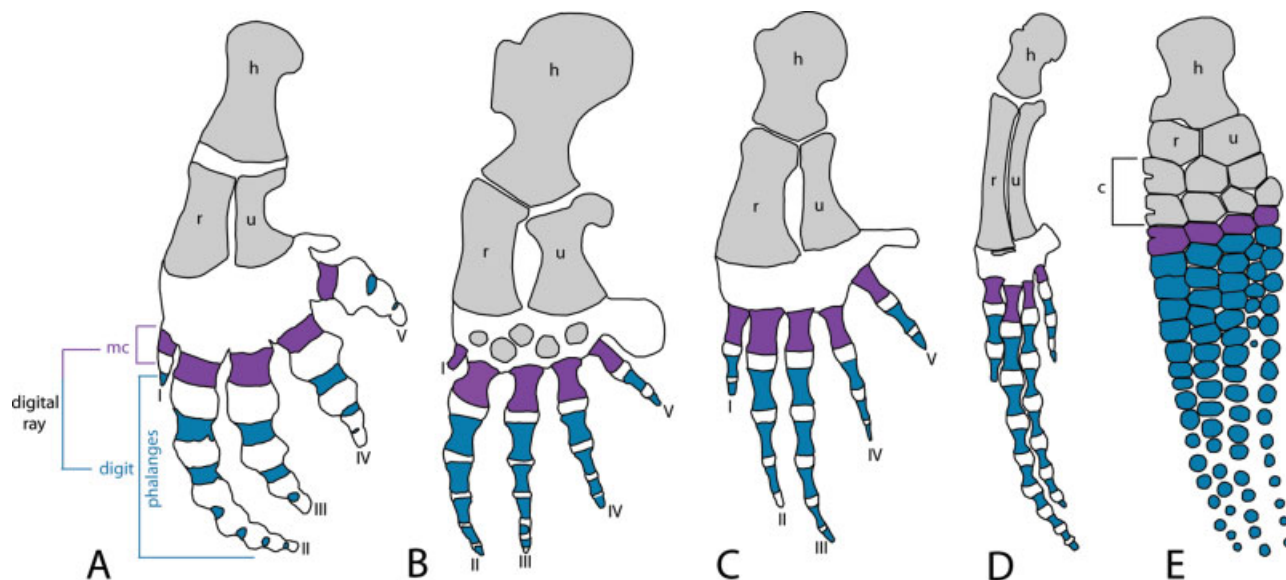


Fig. 1. Hyperphalangy in modern cetaceans and a Mesozoic marine ichthyosaur, *Stenopterygius* (Caldwell, 2002). A digit is made of phalanges, while a digital ray is made of both phalanges and a metacarpal. Roman numerals indicate digit and digital ray identity. **A:** Killer

whale (*Orcinus orca*). **B:** Sperm whale (*Physeter macrocephalus*). **C:** North Atlantic right whale (*Eubalaena glacialis*). **D:** Humpback whale (*Megaptera novaeangliae*). **E:** fossil ichthyosaur (*Stenopterygius*). c, carpal elements; h, humerus; mc, metacarpals; r, radius; u, ulna.

Although the origin of tetrapods is associated with their emergence from the sea (Clack, 2002), many tetrapods have returned to the water. An exceptional fossil record documents the limb-to-fin transition in several extinct lineages of marine tetrapods, including Mesozoic reptiles such as mosasaurs, ichthyosaurs, plesiosaurs, and pliosaurs (Caldwell, 2002). In many lineages of aquatic tetrapods including marine mammals (e.g., pinnipeds, sirenians, and cetaceans), fossils document the evolutionary changes from a weight-bearing forelimb, to a limb encased in a soft tissue flipper used in aquatic locomotion. In mosasaurs, the large and broad flipper allowed at least partial lift-based propulsion and the ability to swim quickly with high maneuverability (O'Keefe, 2001). However, in cetaceans (whales, dolphins, and porpoises) the flippers are streamlined and elongated, a shape that functions in lift, breaking, turning, and to stabilize and maintain equilibrium while swimming (Fish and Rohr, 1999). Along with the development of a soft tissue flipper, some marine reptiles and cetaceans also developed unique bony morphologies of the manus that support the narrow and elongated flipper shape, namely digit reduction and hyperphalangy.

Hyperphalangy is defined here as an increased number of phalanges per digit beyond the plesiomorphic conditions of 2/3/4/5/4 for all amniotes and more specifically 2/3/3/3/3 for mammals (Richardson and Chipman, 2003; Fedak and Hall, 2004), which evolved from the primitive reptilian formula of 2/3/4/5/3–4 among cynodont synapsids (Richardson and Chipman, 2003). Some extinct marine reptiles exhibit hyperphalangy in all their digits (Fig. 1E, Caldwell, 2002; Richardson and Chipman, 2003; Fedak and Hall, 2004); however hyperphalangy in toothed whales (odontocetes) is mostly restricted to the second and third digits (Fig. 1A,B; Richardson and Oelschläger, 2002).

The cetacean manus has been the focus of numerous descriptive studies documenting the patterns of digit ossification and phalangeal counts in isolated taxa (e.g., Gahr et al., 1982; Benke, 1993; Watson et al., 1994; Calzada and Aguilar, 1996; Ortega-Ortiz and Villa-Ramirez, 2000; Richardson and Oelschläger, 2002; Dawson, 2003; Fedak and Hall, 2004), but only recently has a more synthetic view of digital evolution emerged. Using a limited number of taxa, Fedak and Hall (2004) hypothesized that the derived condition of hyperphalangy (unconventionally defined as exhibiting a phalangeal formula greater than 4/6/6/6/6 which is greater than the earliest known tetrapods and, therefore, represents a new tetrapod morphology) evolved three separate times within cetaceans. While their sample included a limited number of cetacean species, Fedak and Hall (2004) set the stage for a broader and more detailed analysis of cetacean manus evolution.

Several hypotheses have been proposed regarding the developmental mechanisms underlying the acquisition of hyperphalangy (Caldwell, 2002; Richardson and Oelschläger, 2002; Fedak and Hall, 2004) but all remain untested, as the genes expressed during the formation of additional phalanges are unknown in cetaceans. However, a study of digital development in the pantropical spotted dolphin (*Stenella attenuata*) (Richardson and Oelschläger, 2002) revealed that additional phalanges were added to the distal ends of the second and third digits after the apical ectodermal ridge (AER) thickened and became isolated to the distal ends of just these digits. This finding led the authors to speculate that the extended presence of the AER likely determines the number of phalanges. Ultimately, Richardson and Oelschläger (2002) inferred this pattern of distal phalangeal addition and AER localization to be caused by heterochronic prolonged limb outgrowth. This hypothesis is

TABLE 1. Previously published hypotheses of the identity of the absent digit in tetradactylous baleen whales

Reference	Digit	Data/explanation
Turner (1892)	IV	Enlarged caudalmost interdigital space
Kükenthal (1893)	III	Cartilagenous phalanges floating in interdigital space Two branches of radial nerve, rather than one in interdigital space
Flower (1885), Kunze (1912)	I	Disagreed with Kükenthal's (1893) hypothesis No evidence indicating which digit was lost
Howell (1930)	I	Reduced number of phalanges in digit I of pentadactylous baleen whales

consistent with the pattern of manus ossification in *S. attenuata*. Ontogenetically older specimens had a greater number of ossified phalanges, and phalangeal epiphyses were the last parts of the manus to ossify and fuse to their respective diaphyses (Calzada and Aguilar, 1996).

As with hyperphalangy, digit loss is common in secondarily aquatic tetrapods. Most ichthyopterygian marine reptiles evolved tetradactyly by losing either digit I or V. Motani (1999) hypothesized ichthyosaurs lost digit I based on the ossification sequences in extant lizards, crocodiles, and an ontogenetic series of ichthyopterygians. However, based on patterns of digit ossification in fossil ichthyosaurs, Caldwell (1997, 2002) hypothesized that digit V sometimes failed to ossify.

Most mysticete (baleen whale) lineages (Balaenopteridae, Neobalaenidae, and Eschrichtiidae) also only have four digital rays, each consisting of a metacarpal and some phalanges (Fig. 1D), but their homology is unresolved (Table 1). Turner (1892) noted an enlarged interdigital space between the two caudal-most digits in a minke whale (*Balaenoptera acutorostrata*) and hypothesized that this marked the location of the missing digit (Table 1). Kükenthal (1893) hypothesized the loss of digit III based on the presence of cartilaginous remnants in the shape of phalanges (histology of these elements showed they were cartilaginous and surrounded by connective tissue) and two branches of the radial nerve, instead of a single nerve, between the middle two digits in multiple specimens of balaenopterids (Table 1). This hypothesis has been accepted by several contemporary researchers (i.e., Barnes and McLeod, 1984; Sedmera et al., 1997; Kato, 2002; Aguilar, 2002) and was supported by similar findings of cartilage remnants in two specimens of fetal balaenopterids (Burfield, 1920). However, Howell (1930) believed Kükenthal's (1893) hypothesis was flawed and that he misidentified metacarpal I as a prepollex and that specimens with the cartilage remnants were likely pathological. The reduced number of phalanges in digit I in pentadactylous baleen whales ultimately led Howell (1930) to argue the loss of digit I in tetradactylous baleen whales. Kunze (1912) also disputed Kükenthal's (1893) hypothesis and assumed that the phalanges appearing in the interdigital space were probably the remnants of a split digit, and he argued that two branches of a single nerve in a single interdigital space was not enough information to hypothesize the loss of digit III. Kunze (1912) added that the sei whale (*Balaenoptera borealis*) displayed two branches of the median nerve in the second interdigital space, and the

two branches of the ulnar nerve innervated the third interdigital space. Flower (1885) also stated that digit I was lost in tetradactylous taxa, but offered no explanation. Surprisingly, several contemporary researchers have assumed that digit V was lost in their osteological descriptions of mysticete taxa (Omura and Kasuya, 1976; Omura et al., 1981; Paterson et al., 1997; Fedak and Hall, 2004). The subject is further complicated by Burfield's report (1920) that multiple species of rorqual mysticetes (balaenopterids) occasionally express a cartilaginous element bearing the same morphology and articulation as the metacarpal I of pentadactylous cetaceans. The presence of this possible metacarpal I was not taken into account in later digit loss hypotheses.

The objective of this study was to conduct a survey of cetacean metacarpal and phalangeal morphologies. The evolution of hyperphalangy was traced in a phylogenetic context and characters were optimized onto previously published cetacean phylogenies. Several digit loss hypotheses (e.g., Flower, 1885; Kükenthal, 1889; Turner, 1892; Kunze, 1912; Howell, 1930) were tested using data from published descriptions, dissections of extant taxa, and examination of osteological specimens and radiographs.

METHODS AND MATERIALS

By means of dissection, carpal elements were examined in 16 cetacean flippers representing 10 species (8 mysticetes, 2 odontocetes) (Table 2). Results were compared with published carpal morphologies in two fossil archaic whales (archaeocetes), *Ambulocetus natans* (Theissen et al., 1996) and *Dorudon atrox* (Uhen, 2004). Because the bones and cartilage of the flipper are slow to mature in extant mysticetes, complete carpal ossification was rarely observed in all examined fresh and published dissections. Museum collections were insufficient for these studies because carpal elements are frequently missing or lack defined articular surfaces due to this lack of ossification. In lieu of examining only the morphology of incompletely ossified and burr-shaped carpal elements in dissections, this study focused on the position of fibrous, uncavitated joints that surround individual carpal cartilages which usually encased a carpal ossification center (Flower, 1885; Eschricht and Reinhardt, 1866). Each fibrous joint indicates where joint cavitation and articular cartilage would form if a complete synovial joint were to develop (Archer et al., 2003). Carpal ossification begins at the center of these

TABLE 2. List of dissected specimens, collection information and approximate ontogenetic age

Taxon	Common name	Specimen ID	Institution	Ontogenetic age
Mysticeti				
Balaenidae				
<i>B. mysticetus</i>	Bowhead	03B11	Barrow Arctic Science Ctr., Barrow, AK	Neonate
<i>B. mysticetus</i>	Bowhead	03B14	Barrow Arctic Science Ctr., Barrow, AK	Neonate
<i>E. glacialis</i>	Right	NY-2680-2001	Smithsonian Institution, Washington, DC ^a	Juvenile
Eschrichtiidae				
<i>E. robustus</i>	Gray	KXD-0060	SW Fisheries Science Ctr., San Diego, CA	Yearling
Balaenopteridae				
<i>B. acutorostrata</i>	Minke	COA 0207171	College of the Atlantic, Bar Harbor, ME	Neonate
<i>B. acutorostrata</i>	Minke	None	Geology Dept., Univ. of Otago, Dunedin, NZ	Juvenile
<i>B. acutorostrata</i>	Minke	MMSC-05-121	Smithsonian Institution, Washington, DC ^a	Mature
<i>B. borealis</i>	Sei	NY-2659-01	Smithsonian Institution, Washington, DC ^a	Mature
<i>B. brydei</i>	Bryde	USNM- 578922	Smithsonian Institution, Washington, DC	Mature
<i>B. physalus</i>	Fin	None	Florida Marine Research Inst., St. Petersburg, FL	Neonate
<i>B. physalus</i>	Fin	USNM- 484994	Smithsonian Institution, Washington, DC	Neonate
<i>B. physalus</i>	Fin	SW-03971	Sea World, San Diego, CA	Neonate
<i>B. physalus</i>	Fin	SYBP-0448	Smithsonian Institution, Washington, DC ^a	Mature
<i>B. physalus</i>	Fin	MMSC-01-016	Smithsonian Institution, Washington, DC ^a	Mature
<i>M. novaeangliae</i>	Humpback	NY-2700-2001	Smithsonian Institution, Washington, DC ^a	Neonate
Odontoceti				
Physeteridae				
<i>P. macrocephalus</i>	Sperm	WJW-003	Smithsonian Institution, Washington DC ^a	Mature
<i>Orcinus orca</i>	Orca	S-946	San Diego St. Univ., San Diego, CA	Adult

^aSpecimens were originally at the Mount Sinai School of Medicine, NY, and transferred to the Smithsonian Institution to be part of the permanent collection.

cartilages and radiates toward the fibrous joints lining the perimeter of each carpal cartilage (Archer et al., 2003). By examining the position of these fibrous joints, the number of carpal elements could be determined, and the carpal–carpal and carpometacarpal articulations could be identified.

Published reports of carpal element morphologies reveal considerable variability within the carpus of odontocetes (i.e., Flower, 1885; Kunze, 1912; Eales, 1954; Yablokov, 1974; Gihl et al., 1982), but a reasonably stable morphology within mysticetes (i.e., Flower, 1885; Burfield, 1920). This stable mysticete morphology is to display a total of six carpals, with four carpal elements in the proximal row nearest the radius and ulna, and two elements in the distal row (Fig. 2E–J). Information was collected from published reports of all cetacean carpal morphologies, but focused on those taxa that displayed the mysticete-like condition of six elements.

Historically, terminology of the forelimb orientation and individual forelimb elements vary in cetacea studies, and here we use the standard *Nomina Anatomica Veterinaria* (International Committee on Veterinary Gross Anatomical Nomenclature, 2005) nomenclature. For orientation, the leading edge of the flipper is referred to as “cranial,” and the trailing edge as “caudal,” and the two main surfaces of the flipper are termed “dorsal” or “palmar.” The term “digit” is used when referring to only the phalanges that make up a finger, while the term “digital ray” is used when referring to the metacarpal and all phalanges of a finger (Fig. 1). Carpal (C) element terminology was supplemented with minor additions to account for element fusion and terminology used for fossil cetaceans (Table 3). The proximal row of carpal elements in a cranial to caudal direction, are here referred to as the scaphoid, lunate, cuneiform, and pisiform as in archaeocetes. The two elements of the

distal row are here referred to as the trapezoid, and unciform (Flower, 1885). The unciform is believed to be the fusion of C4 and C5 (Eales, 1954; Gihl et al., 1982; Rommel, 1990). The trapezium (C1) is lost in extant cetaceans by fusion with metacarpal I and never appears as a distinct element, although metacarpal I frequently assumes the shape of a carpal element in odontocetes (Flower, 1885). The magnum (C3) was lost or fused with the trapezoid (C2; Gihl et al., 1982).

Disarticulated and unlabeled metacarpals and phalanges are frequently preserved in museum osteological collections. Because of a lack of distinguishing characteristics and their similarity in size, it is nearly impossible to reliably distinguish between metacarpal and phalangeal elements, sequential elements of the same digit, or elements of different digits in disarticulated osteological specimens. Furthermore, distal elements are frequently lost in preparation because of their minute size. Radiographs of cetacean flippers offer a precise means of accurately counting the number of bony elements per digital ray in situ as radiographs are taken of whole flippers before maceration. For each radiograph, the numbers of ossified metacarpal and phalangeal diaphyses were counted for each digital ray, regardless of the size of the ossified element. The distal-most ossified phalangeal diaphysis was counted as the terminal phalanx.

A large sample of cetacean flipper radiographs (36 odontocetes and 5 mysticetes) from the collections of the Los Angeles County Museum (LACM) and Smithsonian Institution (USNM) marine mammal collections were photographed (Appendix). Number and placement of metacarpals and phalanges per ray were recorded (Tables 4, 5). Samples represent all cetacean families except the monotypic Lipotidae. Because odontocetes strand frequently and because their forelimbs are small and easy to handle, most museum radiographic collec-

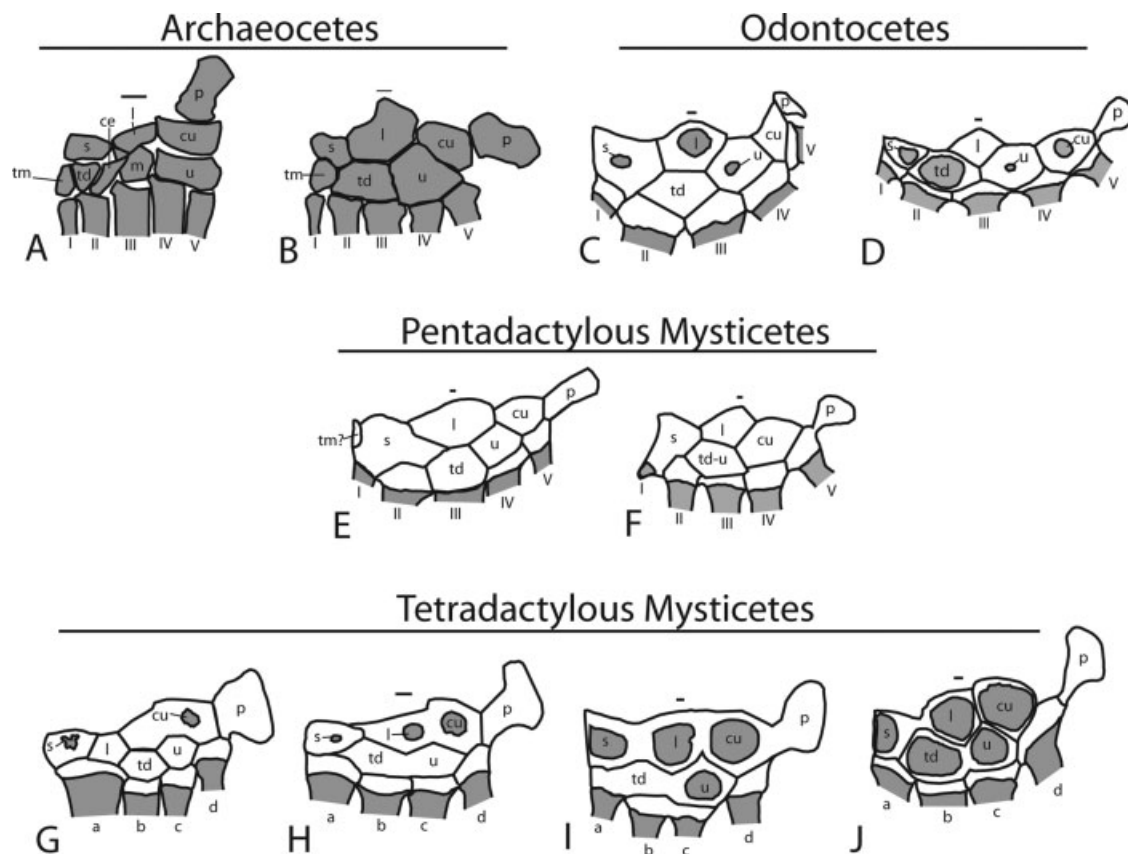


Fig. 2. Wrist morphology in various cetaceans indicating cartilage in white and bone in gray. The cranialmost metacarpal is to the left. Metacarpal identity is shown in roman numerals. Because digital ray homology is unknown in tetradactylous taxa, metacarpal identity is indicated as a–d. **A:** Archaeocete *Ambulocetus* (Thewissen et al., 1996). **B:** Archaeocete *Dorudon* (Uhen, 2004). **C:** Killer whale. **D:**

Sperm whale. **E:** northern right whale. **F:** Bowhead. **G:** Humpback (Struthers, 1889). **H:** Minke whale. **I:** Fin whale. **J:** Sei whale. cu, cuneiform; ce, centrale; l, lunate; m, magnum; p, pisiform; s, scaphoid; td, trapezoid; tm, trapezium; u, unciform. Scale bar = 1 cm in all taxa except G, which is not to scale.

TABLE 3. Nomina Anatomica Veterinaria (Int. Comm. Vet. Gross Anat. Nomen., 2005) terminology of carpal elements, and additional terms from the literature shown in parentheses

Proximal row	Distal row
Os centrale	Os carpale I = Os trapezium
Os radiale = Os scaphoideus	Os carpale II = Os trapezoideum
Os intermedium = Os lunatum	Os carpale III = Os capitatum (magnum)
Os ulnare = Os triquetrium (cuneiform)	Os carpale IV = Os hamatum
Os accessorium = Os pisiforme	(Carpale IV fused to Carpale V = unciform)

tions are greatly skewed with an abundance of odontocete radiographs. Furthermore, mysticete forelimbs are typically too large to radiograph with ease, therefore, radiographs from these whales are from immature specimens. Metacarpal and phalangeal counts were also gathered from a literature survey.

Digital ray elements of eight articulated osteological mysticete forelimbs were counted and photographed at the following institutions: Smithsonian Institution (USNM),

American Museum of Natural History (AMNH), Museo di Storia Naturale del Territorio, dell'universita di Pisa, Italy (MSNT), and National Science Museum, Tokyo, Japan (NMST). Specimens exhibiting humeral epiphyseal fusion were included; however, as the manus of a mature pygmy right whale (*Caperea marginata*) was unavailable, an immature specimen was included in the analysis but was also supplemented with a phalangeal count from the literature (Table 5).

Using phalangeal count data (not metacarpal data) obtained from radiographs, articulated osteological specimens, dissected specimens, and the literature, the mode of phalangeal counts was tabulated for each digit. Modal data were then coded in a MacClade 4.0 character matrix (Maddison and Maddison, 2000).

Developmental studies have shown phalanges are added to the distal ends of digits (e.g., Calzada and Aguilar, 1996; Richardson and Oelschläger, 2002). Modal data were, therefore, coded as ordered characters, 0 (phalanges absent), 1 (proximal phalanx) in succession to 13 (our recorded maximum number of phalanges). In some cases, the most frequent value was tied between two numbers (i.e., four and five) and the number entered was the lower value (in this case four) to give the most conservative estimate of phalangeal elements. It was

TABLE 4. Metacarpal and phalangeal counts for odontocete taxa

Taxon ^a	Digital ray I		Digital ray II		Digital ray III		Digital ray IV		Digital ray V		Reference
	mc	ph	mc	ph	mc	ph	mc	ph	mc	ph	
Physeteridae											
<i>P. macrocephalus</i> (6)	1	0-1	1	3-6	1	4-5	1	2-4	1	0-3	This study; Flower (1868); Benke (1993)
Kogiidae											
<i>K. breviceps</i> (13)	1	1-2	1	7-8	1	6-7	1	5-6	1	3-5	This study; Benke (1993)
<i>K. simus</i> (7)	1	1-2	1	6-8	1	6-8	1	4-6	1	3-5	This study
Ziphiidae											
<i>B. bairdii</i> (2)	1	1	1	4	1	3	1	2-3	1	2	Flower (1872), Grassé (1967)
<i>Hyperoodon</i> (2)	1	1	1	5-6	1	5-6	1	3-4	1	1-2	Turner (1892); Grassé (1967)
<i>Mes. bidens</i> (3)	1	0-1	1	5	1	4-5	1	3-4	1	2	Turner (1885); Turner (1908)
<i>Mes. densirostris</i> (2)	1	0	1	5-6	1	5-6	1	3-4	1	2	This study
<i>Mes. europaeus</i> (9)	1	0	1	5-6	1	5-6	1	4	1	2-3	This study
<i>Mes. hectori</i> (2)	1	0-1	1	5	1	5	1	3-4	1	2	This study
<i>Mes. mirus</i> (4)	1	0	1	4-7	1	4-6	1	3-4	1	2	This study
<i>Mes. stejnegeri</i> (2)	1	0-1	1	4-5	1	4-5	1	3-4	1	1-2	This study
<i>Mes. bidens</i> (3)	1	0-1	1	5	1	4-5	1	3-4	1	2	Turner (1885); Turner (1908)
<i>Mes. densirostris</i> (2)	1	0	1	5-6	1	5-6	1	3-4	1	2	This study
<i>Ziph. cavirostris</i> (1)	1	1	1	3	1	4	1	4	1	2	This study
Platanistidae											
<i>Plat. gangetica</i> (14)	1	1-2	1	3-5	1	3-4	1	3-5	1	3-5	This study; Turner (1908); Pilleri and Gihir (1976a); Gihir et al. (1982)
Iniidae											
<i>I. geoffrensis</i> (13)	1	0-2	1	4-8	1	4-5	1	2-4	1	1-3	Grassé (1967); Fitzgerald (1970); Pilleri and Gihir (1976c); Gihir et al. (1982); Benke (1993)
Pontoporiidae											
<i>Pont. blainvilliei</i> (25)	1	0	1	4-5	1	3-5	1	2-3	1	2-3	This study; Pilleri and Gihir (1976b); Gihir et al. (1982)
Monodontidae											
<i>Mon. monoceros</i> (5)	1	1-2	1	3-6	1	4	1	2-3	1	2	This study; Turner (1908); Eales (1954) Benke (1993)
<i>D. leucas</i> (5)	1	1	1	3-6	1	3-4	1	2-4	1	1-3	This study; Turner (1908); Grassé (1967); Benke (1993)
Phocoenidae											
<i>N. phocaenoides</i> (2)	1	1-2	1	7	1	6-7	1	3	1	1-2	Allen (1923); Benke (1993)
<i>Pho. phocoena</i> (27)	1	0-2	1	5-9	1	5-8	1	2-4	1	0-2	This study; Benke (1993); Dawson (2003)
<i>Pho. sinus</i> (9)	1	1	1	7-8	1	6-7 (0-3) ^b	1	2-4	1	1-2	Fitzgerald (1970); Ortega-Ortiz et al. (2000)
<i>Pho. spinipinnis</i> (1)	1	1	1	6	1	6	1	3	1	0	this study
<i>Phocoen. dalli</i> (2)	1	1	1	6	1	4-5	1	1-2	1	1	this study; Fitzgerald (1970)
Delphinidae											
<i>Ceph. commersoni</i> (2)	1	0	1	6	1	4-5	1	2-3	1	2	This study
<i>Ceph. hectori</i> (1)	1	0	1	5	1	4	1	2	1	0-1	This study
<i>Ceph. heavisidii</i> (1)	1	2	1	7	1	4-5	1	3	1	1	This study
<i>D. delphis</i> (72)	1	0-2	1	7-9	1	5-7	1	2-4	1	0-2	This study; Turner (1908); Grassé (1967) Fitzgerald (1970); Benke (1993)
<i>F. attenuata</i> (2)	1	1-2	1	7	1	6	1	2-3	1	1-2	This study; Fitzgerald (1970)
<i>Gram. griseus</i> (10)	1	0-2	1	7-9	1	6-7	1	2-3	1	0-2	This study; Turner (1908); Grassé (1967); Fitzgerald (1970)

TABLE 4. Metacarpal and phalangeal counts for odontocete taxa (continued)

Taxon ^a	Digital ray I		Digital ray II		Digital ray III		Digital ray IV		Digital ray V		Reference
	mc	ph	mc	ph	mc	ph	mc	ph	mc	ph	
<i>Gl. macrorhynchus</i> (8)	1	0-2	1	8-10	1	6-8	1	1-3	1	0-1	This study; Lee (1978)
<i>Gl. melaena</i> (5)	1	2-3	1	12-13	1	8	1	2	1	0-1	This study; Flower (1885); van Beneden and Gervais (1868); Gahr et al. (1982)
<i>Lag. acutus</i> (44)	1	1-2	1	7-10	1	5-6	1	2-4	1	0-2	This study; Benke (1993)
<i>Lag. albirostris</i> (3)	1	0	1	9	1	6-7	1	3	1	0-2	This study; Turner (1908); Benke (1993)
<i>Lag. cruciger</i> (1)	1	2	1	7	1	5	1	1	1	0	Benke (1993)
<i>Lag. hosei</i> (2)	1	0	1	5-7	1	4-5	1	2	1	0	This study; Benke (1993)
<i>Lag. obliquidens</i> (9)	1	1-2	1	8-9	1	5-6	1	2-3	1	1-2	This study; Fitzgerald (1970)
<i>Lag. obscurus</i> (1)	1	1	1	9	1	6	1	2	1	1	Benke (1993)
<i>Liss. borealis</i> (6)	1	1	1	7	1	5	1	2-3	1	2-3	This study; Fitzgerald (1970)
<i>Orcinus orca</i> (3)	1	0-2	1	4-6	1	3-4	1	3	1	0-2	Grassé (1967); Benke (1993); S-946
<i>Pep. electra</i> (1)	1	2	1	8	1	5	1	3	1	2	Fitzgerald (1970)
<i>Pseu. crassidens</i> (17)	1	0-1	1	4-8	1	4-6	1	1-3	1	0-1	Grassé (1967); Gahr et al. (1982)
<i>Sot. fluvialtilis</i> (55)	1	0	1	6-8	1	3-5	1	2-8	1	1-3	Grassé (1967); Fitzgerald (1970); Benke (1993); Menezes and Simões-Lopes (1996)
<i>Sten. attenuata</i> (7)	1	1	1	7-8	1	4-6	1	1-2	1	0-1	This study
<i>Sten. clymene</i> (8)	1	0-2	1	7-10	1	5-7	1	2-4	1	0-2	This study
<i>Sten. coeruleoalba</i> (21)	1	0-2	1	6-9	1	5-7	1	2-3	1	0-2	This study
<i>Sten. frontalis</i> (6)	1	0-2	1	6-8	1	4-6	1	1-2	1	0-2	This study
<i>Sten. longirostris</i> (5)	1	0-1	1	7-9	1	5-6	1	2-3	1	0-1	This study
<i>Sten. plagiodon</i> (2)	1	1	1	8	1	6	1	2	1	0-1	This study
<i>Steno bredanensis</i> (15)	1	1-2	1	6-8	1	4-6	1	1-3	1	1-2	This study; Grassé (1967); Fitzgerald (1970)
<i>T. truncatus</i> (82)	1	0-1	1	5-8	1	5-6	1	2-4	1	0-2	Benke (1993); Watson et al. (1994)
<i>Sten. longirostris</i> (5)	1	0-1	1	7-9	1	5-6	1	2-3	1	0-1	This study

mc, metacarpal; ph, phalanges.

^aSample sizes are shown in parentheses.^bA supernumerary digit with a maximum of three phalanges has become a fixed trait for *Pho. sinus*.

TABLE 5. Metacarpal and phalangeal counts for mysticete taxa

Taxon ^a	Digital ray I		Digital ray II		Digital ray III		Digital ray IV		Digital ray V		Reference
	mc	ph	mc	ph	mc	ph	mc	ph	mc	ph	
Balaenidae											
<i>B. mysticetus</i> (9)	1	0–2	1	3	1	4–5	1	3	1	2	This study; Eschricht and Reinhardt (1866); van Beneden and Gervais (1868); Flower (1885); Grasse (1967); Albert (1981); Benke (1993)
<i>E. australis</i> (3)	1	0–2	1	3–4	1	4–5	1	4	1	3	Grassé (1967); van Beneden and Gervais (1880); Benke (1993)
<i>E. glacialis</i> (3)	1	1–2	1	4	1	4–5	1	2–3	1	2–3	AMNH 42752; MSNT 264; Benke (1993)
<i>E. japonica</i> (2)	1	1–2	1	4	1	5	1	3–4	1	2–3	USNM 339990; Omura et al. (1969)
Neobalaenidae											
<i>C. marginata</i> (2)	0	0	1	2–4	1	3–5	1	3–4	1	1–3	AMNH 036692; Grassé (1967)
Eschrichtiidae											
<i>E. robustus</i> (6)	0	0	1	2–3	1	4–5	1	3–4	1	2–3	This study; Albert (1981)
Balaenopteridae											
<i>B. acutorostrata</i> (3)	0	0	1	3	1	6–7	1	5–6	1	3	USNM 49775; Turner (1892); Grassé (1967)
<i>B. bonaerensis</i> (3)	0	0	1	4–5	1	6–7	1	5–7	1	3–4	Omura and Kasuya (1976); Arnold et al. (1987)
<i>B. borealis</i> (10)	0	0	1	3–4	1	5–7	1	4–7	1	2–4	Struthers (1889); Schulte (1916); Grassé (1967); van Beneden and Gervais (1880)
<i>B. brydei</i> (1)	0	0	1	4	1	6	1	6	1	2–3	Omura et al. (1981)
<i>B. musculus</i> (6)	0	0	1	3–4	1	5–8	1	5–7	1	3–4	USNM 124326; Struthers (1889); Grassé (1967)
<i>B. m. brevicauda</i> (1)	0	0	1	3–4	1	5	1	4–5	1	2	Omura et al. (1970)
<i>B. omurai</i> (1)	0	0	1	5	1	7	1	6	1	2	NMST-M32505
<i>B. physalus</i> (1)	0	0	1	2	1	5	1	5	1	3	this study; AMNH 035026; Grassé (1967)
<i>M. novaengliae</i> (3)	0	0	1	2	1	7–8	1	6–7	1	2–3	van Beneden and Gervais (1880); Kükenthal (1893); Struthers (1889)

^aSample sizes are shown in parentheses. Most mysticete phalangeal counts come from immature specimens.

noted that the plesiomorphic condition in mammals, including archaeocetes (Thewissen et al., 1996; Uhen, 2004) is 2/3/3/3/3, but polarization was not assigned. Therefore, character states were coded as ordered but not polarized. The resulting tree, therefore, hypothesizes genealogical relationships between states, or hypothesizes synapomorphies (Wilkinson, 1992).

Character states were optimized onto two phylogenies. Because the current published literature lacks a species-level cetacean phylogeny, two trees were used. For odontocetes, the combined morphological and molecular tree of Messenger and McGuire (1998) was used. For mysticetes, recent studies based on mtDNA and nuclear DNA sequences (Rychel et al., 2004; Sasaki et al., 2005), and insertions of transposons (Nikaido et al., 2006) yield generally consistent results among taxa. To accurately trace

the evolutionary history of hyperphalangy, character states were optimized onto both topologies in MacClade 4.0 (Maddison and Maddison, 2000) using ordered characters and the ACCTRAN option. ACCTRAN favors reversals over parallelisms by accelerating transformations toward the root of a tree and is a more conservative means of estimating character transformations in the evolution of hyperphalangy (Maddison and Maddison, 2000).

Because cetaceans differ in their degree of phylogenetic relatedness, it cannot be assumed that samples are independent due to phylogenetic inertia, which may similarly constrain related taxa (Felsenstein, 1985). Cetacean taxa were, therefore, analyzed using independent contrasts (Felsenstein, 1985) in the program Compare 4.5 (Martins, 2004). Pearson's R correlation and associ-

TABLE 6. Odontocete phalangeal correlation values and corresponding *p*-values shown in parentheses^a

	DIGIT I	DIGIT II	DIGIT III	DIGIT IV	DIGIT V
DIGIT I	–				
DIGIT II	0.533 (0.05)	–			
DIGIT III	0.424 (0.130)	0.856 (0.000)	–		
DIGIT IV	0.183 (0.531)	0.125 (0.670)	0.253 (0.383)	–	
DIGIT V	0.112 (0.704)	0.085 (0.773)	0.090 (0.759)	0.318 (0.268)	–

^aThe only statistically significant correlation is shown in bold text.

TABLE 7. Mysticete phalangeal correlation values and corresponding *p*-values (shown in parentheses)^a

	DIGIT I	DIGIT II	DIGIT III	DIGIT IV	DIGIT V
DIGIT I	–				
DIGIT II	0.283(0.372)	–			
DIGIT III	0.183(0.568)	0.137(0.671)	–		
DIGIT IV	0.149(0.643)	0.182(0.572)	0.873(0.000)	–	
DIGIT V	0.332(0.291)	0.069(0.832)	0.303(0.339)	0.283(0.373)	–

^aThe only statistically significant correlation is shown in bold text.

ated *P* values are reported to illustrate which pairs of most similar digits change the number of phalanges (Tables 6, 7). Degree of significance was measured using the adjusted Bonferonni test (Rice, 1988).

RESULTS

A series of consistent articulation patterns were noted by comparing carpometacarpal joints in dissected (fresh and published) cetaceans bearing the mysticete-like morphology of six carpal elements (Fig. 2; Table 8). Because the homology of metacarpals was unknown in tetradactylous taxa, each metacarpal was labeled a–d cranio-caudally (e.g., the cranial-most metacarpal was labeled “a”). Several carpometacarpal joints showed an unambiguous and consistent pattern of articulation between pentadactylous and tetradactylous extant cetaceans, while some other articulations had a less precise relationship between the two groups (Fig. 2; Table 8). Metacarpal I articulates with the cranial articular facet of the scaphoid in all pentadactylous cetaceans, while all tetradactylous taxa lack an element attaching to the scaphoid cranial facet. However, two rorquals, the fin whale (*Balaenoptera physalus*) and humpback whale (*Megaptera novaeangliae*) (Fig. 3) that typically display only four metacarpals, had a cartilaginous element morphologically identical to metacarpal I of the pentadactylous taxa. Metacarpal II articulates with the distal articular facet of the scaphoid and the cranial articular facet of the trapezoid in all pentadactylous taxa, and in tetradactylous taxa, these facets articulate with the cranial-most metacarpal (a). Metacarpal III articulates with the distal articular facet of the trapezoid in pentadactylous mysticetes, but in odontocete taxa metacarpal III articulates instead with the caudal facet of the trapezoid. In all tetradactylous mysticetes, the trapezoid distal articular facet articulates with metacarpal (b). Metacarpal IV articulates with the distal articular facet of the unciform in all pentadactylous taxa, except in the bowhead (*Balaena mysticetus*), which is missing a separate unciform. While it is likely the unciform is fused to the trapezoid, it may also have become fused to the enlarged

cuneiform. It is unclear which element metacarpal IV would articulate with if the unciform were not fused, but it probably would be the unciform distal articular facet as in all other pentadactylous taxa. In all tetradactylous taxa, metacarpal (c) articulates with the unciform distal articular facet. Metacarpal V of pentadactylous taxa articulates with the caudal articular facet of the cuneiform and the distal articular facet of the pisiform. Tetradactylous taxa attach the caudalmost metacarpal (d) with both of these articular facets.

Metacarpals are the proximal-most elements of a digital ray, therefore, digital ray identities were established based on the carpometacarpal articulations (Fig. 4). In tetradactylous taxa, the cranial-most metacarpal (a) was found to share the same articulation as metacarpal II in pentadactylous taxa. Therefore, metacarpal (a) was assigned as equivalent to metacarpal II, and by extension is associated with digital ray II. Metacarpals (b) and (c) of a majority of tetradactylous mysticetes corresponded with metacarpals III and IV in pentadactylous cetaceans. Metacarpals (b) and (c) were, therefore, assigned as equivalent to metacarpals III and IV, and by definition indicate the positions of digital rays III and IV, respectively, in tetradactylous taxa. Lastly, metacarpal (d) shares an identical carpometacarpal articulation with metacarpal V of pentadactylous taxa. Metacarpals (d) and V were, therefore, both assigned as equal and, thus, indicate the position of digital ray V in tetradactylous mysticetes.

A unique carpal arrangement was found in a single specimen of the humpback (*Megaptera novaeangliae*) (Fig. 3). This taxon exhibited an additional carpal between the lunare and the cuneiform in the proximal row, and an extra triangular cartilage articulating with the scaphoid (Fig. 3). This element resembles metacarpal I in its articulation with the proximal carpus and morphology. Burfield (1920) illustrated two specimens of the fin whale (*B. physalus*) with this additional metacarpal I and stated that this element was frequently seen in balaenopterids, although we know of no other documented appearances of this element.

Phalangeal counts were recorded for each digital ray (Tables 4, 5). Odontocetes and mysticetes show differing

TABLE 8. Carpo-metacarpal articulations in pentadactylous and tetradactylous cetaceans bearing the mysticete-like pattern of four proximal and two distal carpal elements^a

Pentadactylous taxa	Cranial scaphoid	Distal scaphoid	Caudal cuneiform	Distal cuneiform	Distal pisiform	Cranial trapezoid	Distal trapezoid	Distal unciform	Caudal unciform	Reference
<i>Ambulocetus</i>	-	-	-	-	-	-	II	IV, V	-	Thewissen et al. (1996)
<i>Dorudon</i>	-	-	-	-	-	-	II, III	IV, V	-	Uhen (2004)
<i>O. orca</i>	I	II	V	IV	V	II	Absent	Absent	IV	This study
<i>Physeter</i>	I	II	V	Absent	V	II	Absent	Absent	IV	This study
<i>P. phocoena</i>	I	II	V	Absent	V	II	Absent	IV	V	Kunze (1912), Eales (1954)
<i>E. glacialis</i>	I	II	V	Absent	V	II	III	IV	V	This study
<i>B. mysticetus</i>	I	II	V	IV	V	II	III	III ^c	IV	This study
Tetradactylous taxa										
<i>M. novaeangliae</i>	-	a	d	d	d	a	b	c	d	Struthers (1889)
<i>M. novaeangliae</i>	-	a	-	d	d	a	b	c	d	Kükenthal (1893)
<i>B. acutorostrata</i>	-	a	d	d	d	a	b	c	d	This study
<i>B. physalis</i>	-	a	d	Absent	d	a	b	c	d	This study
<i>B. borealis</i>	-	a	d	Absent	d	a	b	c	d	This study
<i>B. musculus</i>	-	a	d	d	d	a	b	c	d	Kükenthal (1893)
<i>B. physalus</i> ^b	*	a	d	Absent	d	a	b	c	d	Burfield (1920)
<i>M. novaeangliae</i> ^b	*	a	d	Absent	d	a	b	c	d	This study

^aMetacarpal identity is indicated by roman numerals (mcl = I, etc.). Because digit identity is unknown in tetradactylous taxa, digits are labeled cranio-caudally (a-d). Each articulation is labeled based on the carpal articular facet orientation: cranial, caudal, or distal. In tetradactylous taxa, the scaphoid lacks a cranial articular facet attaching to metacarpal I.

^bSpecimens with an additional element attaching to the cranial articular facet of the scaphoid.

^cThe trapezoid and unciform are fused in *B. mysticetus*.

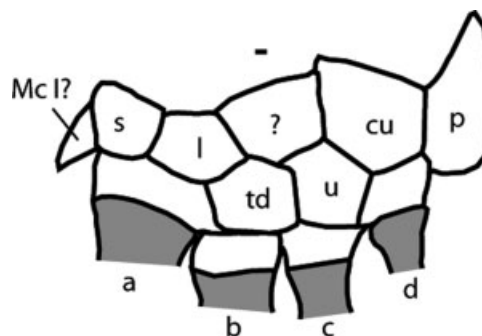


Fig. 3. Wrist morphology of the humpback with two uncommon elements, an additional carpal element (?), and an anterior element that bears the same morphology and articulation as metacarpal I of pentadactylous extant cetaceans (Fig. 2C-F). Abbreviations as in Figure 2. Scale bar = 1 cm.

patterns of phalangeal reduction and hyperphalangy. Digit I has a reduced number of phalanges in most mysticetes and odontocetes, except some specimens of the longfinned pilot whale (*Globicephala melaena*), which exhibit digit I hyperphalangy. Within odontocetes, digits II and III display the greatest degree of hyperphalangy, whereas mysticetes exhibit the greatest degree of hyperphalangy in digits III and IV. Odontocetes display some hyperphalangy in digit IV, but a majority of the taxa retain the plesiomorphic state of three phalanges or counts close to that. Most odontocetes reduce the number of phalanges in digit V. Exceptions are those cetaceans that exhibit hyperphalangy of digit V, such as the beluga (*Delphinapterus leucas*), pygmy sperm whale (*Kogia breviceps*), and Ganges river-dolphin or susu, (*Platanista gangetica*). Most mysticetes exhibit phalangeal numbers at or near the plesiomorphic condition of digit V.

Characters of modal phalangeal counts were optimized onto two phylogenies for each digit (Fig. 5). In both optimizations, digit I displays the greatest amount of phalangeal count reduction (Fig. 5A,F), with only a single taxon, *Globicephala melaena*, displaying hyperphalangy. Modal phalangeal counts for digits II, III, and IV reveal the greatest disparity between odontocete and mysticete cetaceans. Odontocetes display hyperphalangy in digits II and III (Fig. 5B,C). Delphinids possess the greatest degree of hyperphalangy with 7–13 phalanges in digit II (Fig. 5B) and five to eight phalanges in digit III (Fig. 5C). Contrary to odontocetes, mysticetes show the greatest degree of hyperphalangy in digits III and IV (Fig. 5H,I). Balaenopterids display the greatest number of phalanges with five to seven phalanges in digits III and IV (Fig. 5H,I). Digit V also exhibits an overall trend toward phalangeal count reduction (Fig. 5E), however most balaenopterid mysticetes retain the plesiomorphic condition of three phalanges (Fig. 5J). Only *Kogia* displays digit V hyperphalangy (Fig. 5E).

Modal phalangeal count data for each digit was analyzed using Compare 4.5 (Martins, 2004). for correlations between digits, based on independent contrasts (Tables 6, 7). Within the Odontoceti, only a single pair of digits, II and III, were found to be correlated significantly (Table 6). In mysticete taxa, digits III and IV were correlated significantly (Table 7).

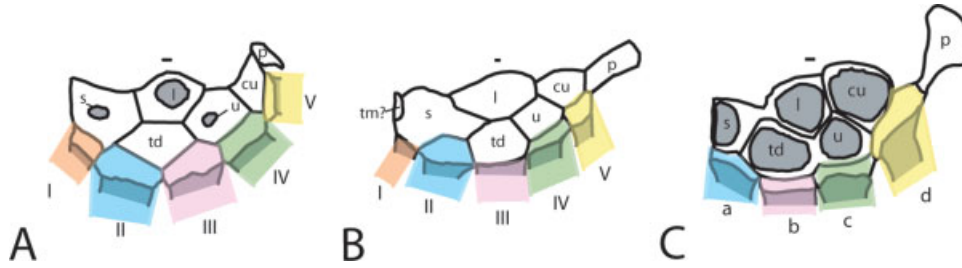


Fig. 4. Hypothesized digital ray homologies based on carpometacarpal articulations. **A:** Pentadactylous odontocete, killer whale. **B:** Pentadactylous mysticete, north Atlantic right whale. **C:** Tetradactylous mysticete, sei whale. Digital ray identities indicated by color: ray I (orange), ray II (blue), ray III (pink), ray IV (green), and ray V (yellow). Tetradactylous mysticetes lack ray I (orange). Scale bar = 1 cm.

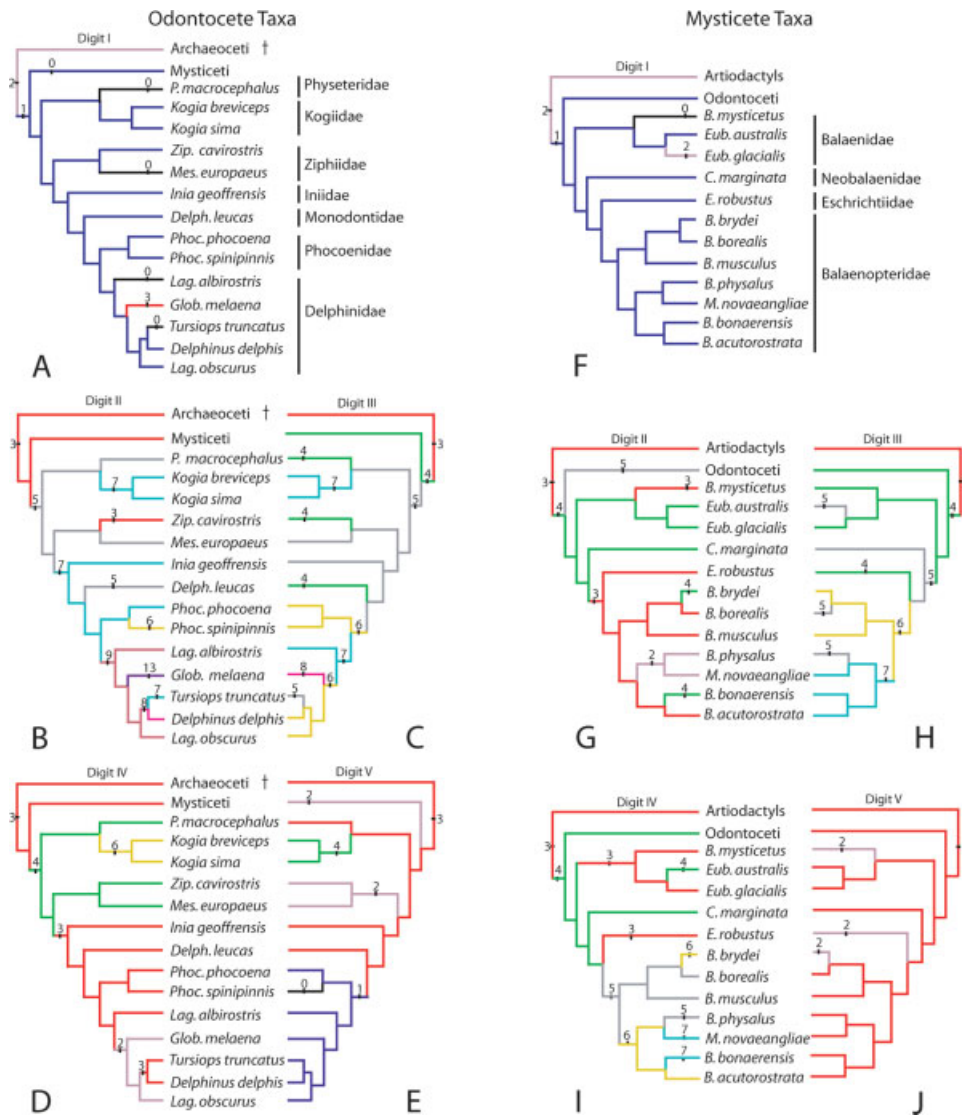


Fig. 5. Phylogenetic distribution of modes of phalangeal counts. **A–E:** Odontocete phalangeal counts optimized onto odontocete phylogeny (Messenger and McGuire, 1998). **F–J:** Mysticete phalangeal counts optimized onto mysticete phylogeny (Rychel et al., 2004; Sasaki et al., 2005; Nikaido et al., 2006). **A,F:** digit I. **B,G:** digit II. **C,H:** digit III. **D,I:** digit IV. **E,J:** digit V.

DISCUSSION

Comparisons

The primitive cetacean wrist morphology is illustrated by the carpus of *Ambulocetus* (Thewissen et al., 1996) and *Dorudon* (Uhen, 2004) in which five metacarpals articulate only with elements of the distal carpal row (Fig. 2A,B). The distal carpal row of *Ambulocetus* is occupied by five carpals, whereas the distal row of *Dorudon* is occupied by three elements. In *Dorudon*, the centrale is absent, the magnum is fused with the trapezoid (Gahr et al., 1982; Uhen, 2004), and the unciform caudal articular facet is steepened to allow metacarpal V to be offset caudally. In extant pentadactylous cetaceans, this morphology persists, and in addition, the trapezium is lost (Flower, 1885) (Fig. 2C–F). Eliminating the trapezium allows metacarpal I to articulate with the cranial facet of the scaphoid in the proximal row. Extant pentadactylous cetaceans have also shifted the metacarpal V articulation proximally to contact the cuneiform and pisiform (Fig. 2).

Both *Ambulocetus* and *Dorudon* have flattened carpometacarpal joints that allow the metacarpals II–IV to abut one another (Fig. 2A,B). Extant odontocete carpals (Fig. 2C,D) display steep cranial and caudal carpal articular facets that afford these metacarpals a large distance between each other and give rise to digits that are more widespread, especially in the orca (*Orcinus orca*) and sperm whale (*Physeter macrocephalus*). Contrary to this morphology, mysticetes display relatively flattened trapezoid and unciform articular facets that articulate with closely appressed metacarpals (Fig. 2G–J). These closely spaced metacarpals give rise to digits that are closely appressed with small interdigital spaces, while only the caudalmost digit is offset toward the trailing edge of the flipper.

In comparing carpometacarpal articulations between pentadactylous and tetradactylous extant cetaceans, our data indicate these articulations are conserved and it is possible to determine digit identity in tetradactylous taxa (Figs. 2, 4). Furthermore, because metacarpals are the most proximal elements of a digital ray, digital ray numbers were designated for each metacarpal. Metacarpal I attaches to the cranial facet of the scaphoid cartilage in all pentadactylous cetaceans, but no metacarpal attaches to this surface in tetradactylous mysticetes. It is, therefore, hypothesized that an ossified metacarpal I, and by definition digital ray I, is absent in tetradactylous taxa.

An exception to this is the cartilage that might be a remnant of metacarpal I found in *M. novaeangliae* (Fig. 3). Struthers (1889) described the carpus of *M. novaeangliae* as having this additional carpal element fused with the cuneiform (Fig. 2G). The additional cartilaginous element articulating with the scaphoid is triangular in shape, and angled craniodistally as in metacarpal I of the pentadactylous taxa, including the northern right whale (*Eubalaena glacialis*), bowhead (*Balaena mysticetus*), killer whale (*Orcinus orca*), sperm whale (*Physeter macrocephalus*), and harbor porpoise (*Phocoena phocoena*) (Kunze, 1912; Eales, 1954) (Fig. 2C–F). Burfield (1920) also illustrated two specimens of the fin whale (*B. physalus*) with this additional possible metacarpal I and stated that this element was frequently seen in balaenopterids, although we know of no other documented appearances of this element.

Metacarpal II in pentadactylous taxa shared identical articulations to metacarpal (a) (Table 8), indicating the position of digital ray II in tetradactylous taxa (Fig. 4). Metacarpal III attaches to the distal surface of the trapezoid in pentadactylous mysticetes, and this articulation also occurs with metacarpal (b) (the metacarpal just caudal to the cranialmost metacarpal), in tetradactylous mysticetes (Table 8; Fig. 4). Metacarpal III of pentadactylous mysticetes is, therefore, thought to be equivalent to this metacarpal in tetradactylous mysticetes. However, this relationship is tentatively proposed because the trapezoid and unciform, or the unciform and cuneiform, are fused in the bowhead and it is unclear where metacarpal (b) would attach in an unfused state. Assignment of metacarpal III equivalence is further complicated by the absence of the trapezoid distal articular facet in examined pentadactylous odontocetes, rendering the tetradactylous articulation an incomparable morphology (Table 8). In addition, the trapezoid appears in a position that replaces the missing articular/growth cartilage at the proximal end of metacarpal III in *E. glacialis* (Fig. 2E). An equally tenuous pattern is seen in the metacarpal IV articulation. It appears that most pentadactylous taxa articulate metacarpal IV with the distal facet of the unciform (Table 8). However, equivalence cannot be definitively stated because of the lack of an unciform fusion in *B. mysticetus*. While it is likely that the unciform is fused to the trapezoid, it is also possible that the unciform has fused with the enlarged cuneiform. This latter condition reflects a consistent articulation of metacarpal IV to the unciform, whether fused (e.g., *B. mysticetus*) or a separate carpal element (e.g., *E. glacialis*). Thus, the pentadactylous mysticete metacarpal IV is considered similar to the tetradactylous mysticete metacarpal (c) (the metacarpal just cranial to the caudalmost digit), which also articulates with the unciform (Fig. 4; Table 8). Metacarpal V articulates with the cuneiform and pisiform in all pentadactylous cetaceans, and this articulation is shared in all tetradactylous taxa, indicating metacarpal V is equivalent to the caudalmost metacarpal in tetradactylous taxa. These hypothesized identities are summarized in Figure 4. Our hypotheses of digital ray identity is based upon similar articulations at the carpometacarpal joints, and these similarities may correspond with homologous digital rays; however, similarity alone is not an effective criterion for assigning homology (Donoghue, 1992).

During this study, we found a unique carpal arrangement in a single juvenile specimen of *Megaptera novaeangliae* that possessed an additional carpal element along the leading edge of the flipper (Fig. 3). The additional carpal element appears to be most similar to ossified metacarpal I of pentadactylous cetaceans and may represent a cartilaginous metacarpal I. Dissection of only a single flipper of *M. novaeangliae* has previously been published (Fig. 2G; Struthers, 1889) and the specimen exhibited a carpal arrangement more similar to other balaenopterids in that it lacked an accessory element articulating solely with the cranial articular facet of the scaphoid. Therefore, it is unclear whether the specimen dissected in this study (Fig. 3) represents a common carpal arrangement, is only representative of the immature condition, or is in fact anomalous. However, of the structures creating leading edge tubercles in the flipper of *Megaptera*, it was noted that this addi-

tional carpal element on the leading edge contributed to a large, proximally placed tubercle, and may have had a direct effect on both flipper shape and the overall hydrodynamic function of the flipper. In the future, further dissection of the manus of additional *M. novaeangliae* specimens may offer insight into distinguishing the common carpal arrangement for this taxon and establish whether *M. novaeangliae* has only four digital rays as in other balaenopterids (Fig. 2G–J), or consistently displays an autapomorphy in the form of an additional digital ray. Because Burfield (1920) described an element of similar morphology and articulation in several specimens of balaenopterids, it is probable that this element simply represents a variable expression of a vestigial metacarpal I in normally tetradactylous mysticetes.

Loss of Digital Ray I

The differing hypotheses of Turner (1892), Kükenthal (1893), and Howell (1930) regarding which digits (IV, III, or I, respectively) were lost in tetradactylous mysticetes were tested based on observations of carpal cartilage arrangements obtained from fresh specimens (Table 1). Turner (1892) noted an enlarged interdigital space in the caudalmost digits of tetradactylous mysticetes, and hypothesized that this space once housed another digit. No data collected in this study indicated a digit was lost along the posterior aspect of the manus. Instead, it appears that metacarpal V initially became caudally offset, leading to a slightly larger fourth interdigital space, in the archaeocete *Dorudon* approximately 40 Ma. However, in extant whales, this caudal offset became even more pronounced as metacarpal V shifted to its current proximal articulation with the cuneiform and pisiform (Fig. 2C–J). Data from this study indicate digital ray V is offset in all pentadactylous cetaceans, not just in tetradactylous mysticetes. Manatees, which are pentadactylous, also show an enlarged interdigital space between digits IV and V (Watson and Bonde, 1986). Turner's (1892) observation of an enlarged caudal-most interdigital space is, therefore, interpreted to indicate a morphology that is likely correlated to the shape of the soft tissue flipper and is, therefore, linked to the flipper function, rather than indicating where a digit was lost. It is, therefore, hypothesized that a slight offset of digital ray V may have first appeared 40 Ma, as illustrated by the morphology of the archaeocete *Dorudon* (Uhen, 2004).

Kükenthal (1893) hypothesized that digit III was lost based on the presence of floating cartilaginous phalanges and the two branches of the radial nerve in the same second interdigital space of some tetradactylous taxa (Table 1). Recent developmental data have shown that interdigital tissues play a large role in the morphogenesis of digital rays, and although the mechanisms are not well understood, both *in situ* and *in vivo* interdigital tissues display a high chondrogenic potential (Sanz-Ezquerro and Tickle, 2003). Phalanges floating in the interdigital space have been experimentally produced by a variety of methods: removing the dorsal ectoderm, removing the interdigital apical ectodermal ridge, and application of a signaling molecule to the interdigital mesenchyme (Sanz-Ezquerro and Tickle, 2003). Sanz-Ezquerro and Tickle (2003) thus hypothesize that the chondrogenic potential of interdigital tissues may contribute to cell migration in forming digit condensations.

The floating digit reported by Kükenthal (1893) should, therefore, be interpreted as a developmental consequence of cetaceans activating the chondrogenic potential of their interdigital tissue in the formation of a soft tissue flipper with intact interdigital tissues, rather than expression of an atavistic digit. Kükenthal (1893) also noted the presence of two branches of the radial nerve, rather than a single nerve, between the middle digits of some tetradactylous mysticetes. Unfortunately, the radial nerve could not be traced in our dissections; however, Weber (1928) noted the presence of two branches of a single nerve within the interdigital space in pentadactylous odontocetes. Kunze (1912) also noted two branches of the median nerve in the second interdigital space, while the third interdigital space displayed two branches of the ulnar nerve in the sei whale. It is important to note that dual branches of the median nerve are common between digits in pentadactylous mammals (Kunze, 1912). Because two branches of a single nerve are present in both pentadactylous cetaceans and pentadactylous terrestrial mammals, a similar nerve innervation in tetradactylous mysticetes does not necessarily indicate the absence of a digit. In this study, we find no evidence digit III was lost. Instead, Kükenthal (1893) and Burfield (1920) were probably reporting the presence of an anomalous, rather than atavistic, floating digit and a common pattern of interdigital nerve innervation for cetaceans.

Howell (1930) considered the floating digit described by Kükenthal (1893) to be pathological and, because digit I is reduced in pentadactylous mysticetes, Howell hypothesized digital ray I was lost in tetradactylous mysticetes. This hypothesis was also proposed by Flower (1885) and Kunze (1912), and they also opposed Kükenthal's (1893) hypothesis, but reported no further data indicating which digit was lost. The hypothesis that digital ray I is absent in tetradactylous taxa is supported based on three lines of evidence gathered from the literature and from data generated in this study. First, in a recent radiographic study of ontogenetically young specimens of *B. mysticetus*, which are typically pentadactylous, Albert (1981) noted the common absence of digital ray I, thus indicating an immature tetradactylous morphology compared with the adult pentadactylous condition. Second, digital ray identifications based on carpometacarpal articulations indicate that tetradactylous mysticetes lack digital ray I, but retain digits II–V in similar articulations with the carpus as in pentadactylous cetaceans. Lastly, there is atavistic expression of metacarpal I in otherwise tetradactylous taxa of *M. novaeangliae* (this study) and *B. physalus* (Burfield, 1920). In general, it is dubious to base digital ray homologies on muscular insertions, as some insertions shift between individuals. Note that, in all pentadactylous cetaceans, the flexor and extensor muscles insert on digits II–V, and in tetradactylous mysticetes, these same muscles insert on all four digits (Cooper et al., *in review*).

Few articulated fossil forelimbs have been described, and the earliest tetradactylous mysticete appears to be preserved in Miocene sediments. *Eobalaenoptera*, the hypothesized earliest representative of the balaenopterid–eschrichiid clade, possessed a forelimb with four digital rays represented by four metacarpals (Dooley et al., 2004). Most phalanges were missing. Given the

age of this fossil balaenopterid, it was concluded that mysticete tetradactyly evolved at least 14 Ma.

Cetaceans are a unique lineage of aquatic tetrapods for which little is known of the developmental aspects of their skeletal manus and fleshy flipper morphologies. However, several other studies document the loss of digit I in a variety of vertebrates. A study of land tortoises (Testudinidae) showed that the loss of digit I had evolved independently among several distantly related land tortoises (Crumly and Sanchez-Villagra, 2004). The authors based their hypotheses of a missing digit I on carpus morphology, but did not test for a developmental mechanism. Instead, they hypothesized digit I was the last to develop based on previously published ontogenetic studies and suggested that the absence of digit I was likely due to heterochrony. In a similar study of the frog manus, Shubin and Alberch (1986) also found that digit I is the last to form.

Within Artiodactyla, the ancestral condition is to have five digits with a reduced digit I in the forelimb, as seen in fossil dichobunids, oreodontids, and anthracotheriids (Stehlin, 1929; Clifford, 2005). The transition to a complete loss of digit I in terrestrial artiodactyls has been correlated with a shift from the primitive digitigrade condition to unguligrady (Clifford, 2005), and all extant terrestrial artiodactyls lack digit I (Vaughan et al., 2000). The fossil archaeocetes *Ambulocetus* and *Rodhocetus* display the primitive artiodactyl condition of five digits, with two phalanges and a single phalanx in digit I, respectively (Thewissen et al., 1996; Gingerich et al., 2001). Most modern cetaceans retain the *Rodhocetus* condition of a reduced number of phalanges in digit I, and also frequently reduce digit V. Moreover, some mysticetes have lost digital ray I (metacarpal I and all phalanges of digit I). Similar patterns of digit reduction have also been documented other lineages of fossil ungulates. The condylarth *Phenacodus* from the late Paleocene and early Eocene displayed reduced digits I and V, and the archaic perissodactyl *Hyracotherium* lacked digit I and displayed a reduced digit V (Carroll, 1988). It appears that the pattern of reducing digital elements along the lateral and medial margins of the manus has occurred in other lineages of ungulates, and is, therefore, not unique to cetaceans.

Developmental studies in vertebrates have shown that the establishment of digit number and identity is controlled by a small group of mesenchymal cells at the caudal margin of the limb bud, called the polarizing region (Sanz-Ezquerro and Tickle, 2003). In general, the identity of a digit depends on its proximity to the polarizing region, with the cranialmost digit being the farthest away. In this model, the polarizing region first induces cells adjacent to it to produce an anterior digit, and then promotes a transformation of this anterior digit into a posterior digit, and initiates formation of a new anterior digit further away (Sanz-Ezquerro and Tickle, 2003). Therefore, digits will be generated in the caudal-to-cranial direction, and digit I will form last. Cells in the polarizing region express the morphogen Sonic hedgehog (*Shh*). As an illustration of the polarizing region activity and *Shh* expression, an immunohistochemical analysis of the Australian lizard *Hemiergis* showed the duration of *Shh* expression corresponded positively to the number of digits formed (Shapiro et al., 2003). Interestingly, digit I condensations failed to appear and, thus, a truncated

expression of *Shh* and a corresponding increase in anterior apoptosis activity were hypothesized as the mechanisms deleting the first digit (Shapiro et al., 2003). The developmental mechanism generating digital ray loss in tetradactylous mysticetes remains unknown, but one explanation may be that tetradactylous mysticetes may have truncated *Shh* expression as in *Hemiergis* (Shapiro et al., 2003), or perhaps a different alteration in protein expression could cause a failure to develop the first digit. However, this will remain an untested hypothesis until developmental studies of the mysticete manus are undertaken.

Evolution of Hyperphalangy

The first large-scale analysis of cetacean hyperphalangy was based on a review of published data (Fedak and Hall, 2004). This study adds new data and differs from Fedak and Hall (2004) in many methods. Here, we use a larger, taxonomically diverse sample of mysticetes and odontocetes. Although both studies optimize character states onto a phylogeny of odontocetes proposed by Messenger and McGuire (1998), the larger sample size of this study provided sufficient data to also trace characters onto a phylogeny of mysticetes (Rychel et al., 2004; Sasaki et al., 2005; Nikaido et al., 2006). This study also uses a different hypothesis of digital ray loss in tetradactylous mysticetes (i.e., loss of digital ray I). A unique arrangement of character states is used to trace the evolution of hyperphalangy. Because developmental data have shown that extra phalanges are added (or lost) to the distal tips of digits, phalanges are ordered from 0 to 13 to accurately reflect this mechanism. Fedak and Hall (2004) traced only the evolution of an extreme form of hyperphalangy that neither offers insight into phalangeal count reduction, nor does it account for metacarpal reduction.

Optimization results from this study indicate little homoplasy in the evolution of cetacean hyperphalangy. Digit I appears to undergo the greatest reduction in phalangeal count (Fig. 5A,F), with hyperphalangy only appearing in the longfinned pilot whale, *Globicephala melaena*. Digits II and III in odontocetes (Fig. 5B,C) and III and IV in mysticetes (Fig. 5H,I) possessed the greatest number of elements. Rather than all cetaceans expressing a larger number of phalanges in these digits, the greatest expression is typically isolated to the later diverging families, delphinid odontocetes and balaenopterid mysticetes. Statistical analyses indicate that these two pairs of digits likely evolved in concert and may be morphologically integrated (Tables 6, 7). Furthermore, it is also reasonable to assume that the mechanism controlling length of digital AER activity is the same in each of these paired digits. However, it appears that the position of the AER activity is located more caudally in mysticetes, as they lack a developed digit I and hyperphalangy is highly expressed in digits III and IV. Few fossil cetacean articulated forelimbs have been described, and the earliest fossil cetaceans exhibiting hyperphalangy appear to be preserved in Miocene sediments. Two specimens of a fossil *Balaenoptera siberi* exhibited hyperphalangy in digits III and IV (Pilleri, 1989, 1990). The fossils display a phalangeal formula of 0/2-4/4-6/5/2 (Pilleri, 1989, 1990) and were excavated from the Aguada de Lomas, of the Pisco formation of

Peru, which has an associated age of 7–8 Ma (Muizon et al., 2003). We, therefore, conclude that hyperphalangy evolved at least 8 Ma in mysticetes.

Future developmental studies may shed light on the hypotheses presented in this study. Although cetacean embryos are difficult to obtain, immunohistochemical analyses may test the hypothesis that ray I was lost in tetradactylous mysticetes and offer insight as to the protein and gene expression associated with hyperphalangy. Furthermore, as more cetacean fossils are described, it is hoped that future authors will include descriptions of the postcranial skeleton and help elucidate the intricacies of cetacean forelimb evolution, including hyperphalangy.

Possible Functional Interpretations

Richardson and Chipman (2003) noted that, in most aquatic animals (except plesiosaurs), the greatest degree of hyperphalangy was documented in species that used their flippers as rudders for steering and balance. Non-plesiosaur Mesozoic marine reptiles and cetaceans may have evolved hyperphalangy in response to hydrodynamic forces placed on the flipper in steering and possibly generating lift. However, there are some notable differences between the hyperphalangeous digits of extant cetaceans and Mesozoic marine reptiles. The articulated fossil forelimbs of ichthyosaurs (e.g., *Stenopterygius* and *Ichthyosaurus*) display ossified phalanges with little to no metacarpophalangeal and interphalangeal joint spaces in the proximal elements, but joint spaces increase toward the distal ends of the digits (Motani, 1999; Caldwell, 2002) (Fig. 1E). This polar spacing of phalanges is consistent throughout ontogeny in these reptile taxa (Caldwell, 2002). Contrary to the morphology seen in Mesozoic marine reptiles, extant cetaceans separate phalanges by large cartilaginous interphalangeal joints that maintain broad spacing along the entire proximodistal axis of the digit (Fig. 1A–D). In some cases, extant cetaceans ossify both epiphyses of metacarpals and phalanges, whereas these epiphyses are lacking in Mesozoic marine reptiles.

The presence of numerous interphalangeal joints may greatly affect the contour of flipper deformation in flexion or extension. With the presence of numerous joints, any digital flexion or extension will create a smooth bow-shaped flipper; whereas an elongated flipper with just long phalanges and fewer joints will produce a digital curvature with more steep angles at each interphalangeal joint. An example of these differing morphologies is illustrated in manus bending in whales versus bats. The hyperphalangeous flipper of a humpback whale bends at numerous smaller angles to create a smooth arc along the length of a digit, while the elongated digits in the wing of bats bend at sharp angles at interphalangeal joints. Similarly, the larger distal interphalangeal joints in Mesozoic marine reptiles may have allowed a smoother flipper contour, while the distal manus bent in flexion or extension. A functional advantage to this morphology is unclear, but it may be advantageous to flex and extend the distal ends of the digits to reduce the magnitude of flipper tip vortices.

Hyperphalangy may also afford the cranial-most digits greater load distribution in responding to high pressure stresses on the leading edge of the flipper. For any given

force acting on the leading edge of the flipper, each interphalangeal joint may absorb some amount of caudally directed force (assuming flow is perpendicular to the longitudinal axis of the flipper) by slightly bending each interphalangeal joint in tension on the leading edge. This would correspondingly cause compression on the trailing edge of the same joints. If each joint only deforms slightly, and the net force is absorbed over several joints, perhaps hyperphalangy may be an efficient means of distributing leading edge forces. Evolutionarily, perhaps hyperphalangy is a functional consequence of having a lift-generating flipper with the greatest pressure on the leading edge surface, as in airfoils.

Hyperphalangy may also just be a consequence of a similar developmental pathway creating both the flippers in Mesozoic marine reptiles and modern cetaceans. It may be that the evolution of hyperphalangy was not selected for, but was a consequence of a mutation associated with the evolution of soft tissue flippers and lift-based swimming. All of these hypotheses remain untested, as no studies have demonstrated functional differences between a manus elongated by the phalangeal lengthening, or elongated by increasing the number of phalanges and interphalangeal joints as generated in hyperphalangy.

With regard to the caudal offset of digital ray V noted by Turner (1892) in balaenopterids, there may be some functional consequences associated with this morphology. The caudally offset digital ray V may function in stabilizing the trailing edge of the flipper, or widening the manus, although no experimental data supports this yet. Taxa with paddle-shaped flippers, (e.g., *Physeter*, *Eubalaena*, *Balaena*, and *Eschrichtius*) display the greatest posterior offset of digital ray V, and it may be that the magnitude of caudal offset correlates with flipper width. In general, more broad flippers are found in taxa that swim at slower speeds (Benke, 1993). Contrary to the morphology seen in the paddle-shaped flippers, balaenopterids have narrow and elongate flippers with digits II–IV tightly appressed and digit V offset only slightly compared with those associated with paddle-shaped flippers.

With regard to possible functional consequences of reducing the number of phalanges per digit as in digit I of pentadactylous cetaceans, or losing digital ray I as in tetradactylous mysticetes, several hypotheses are offered. The flipper is effective at generating lift because of an aspect ratio that is like that of an airplane wing, where the leading edge of the airfoil is subject to the greatest forces compared with the other surfaces of the wing. Perhaps cetaceans have evolved a reduced digit I to minimize forces on an element that already has fewer phalanges. The plesiomorphic mammalian condition is to have only two phalanges in digit I, and cetaceans do have a reduced number of phalanges in digit I. Contrary to this, some Mesozoic marine reptiles have greatly increased the number of phalanges (hyperphalangy) in the first digit, perhaps to further stabilize the leading edge of the flipper. However, tetradactylous mysticetes completely lack digit I and have also lost metacarpal I. This finding may be a consequence of leading edge forces, but the shape of the flipper in most tetradactylous mysticetes also suggests digit loss has greatly affected flipper shape. Both neobalaenids and balaenopterids have narrow and elongate flippers in which the

digits lie closely appressed. Eschrichtiids have only digits II and III closely appressed, but the two caudalmost digits are widely spaced, creating broad flippers that are wider than other tetradactylous mysticetes, but narrow compared with pentadactylous balaenid mysticetes. Tetradactylous mysticetes, therefore, have altered flipper shape by both losing a digital ray, and repositioning the digits relative to each other. We are, therefore, unable to pinpoint a direct functional consequence of digit loss alone, but the absence of a digit in tandem with a repositioning of the digits, may have led to the disparate flipper shapes in mysticete taxa. The narrow and elongate flippers of balaenopterids are probably associated with swimming at high speeds needed for lunge feeding (Goldbogen et al., 2006), whereas the more broad flippers of eschrichtiids and balaenids offer a greater surface area and may aid in low speed turns in shallow lagoons (Benke, 1993).

ACKNOWLEDGMENTS

We thank two anonymous reviewers, J.G.M. Thewissen, C. Vinyard, and P. Reno for commenting on the manuscript. We also thank J.G.M. Thewissen for literature translation and C. Vinyard for statistical and functional assistance. Dissections of fresh specimens were completed with the aid of C.M. Redman, F.E. Fish, V. Naples, K. Kainec, and L. Tomko. We thank V. Naples for housing and assistance during many long dissection hours. We thank J. Mead, C. Potter, D. Allen, and J. Ososky of the Smithsonian Institution, as their contributions have been invaluable in the collection of data of fresh, radiographic, and osteological specimens. We also thank J. Heyning and D. Janiger for use of their radiographic and osteological collections. Fresh specimens were provided by the following stranding agencies and museum collection staff: J.D. Archibald and M. Van Patten, Biology Department, San Diego State University, San Diego, California; S.R. Rommel and A. Costidis of the Florida Marine Research Institute, St. Petersburg, Florida; C. George and M. Irinaga of the Barrow Arctic Science Center, Barrow, Alaska; J. Allen of the College of the Atlantic in Bar Harbor, Maine; E. Fordyce, Geology Department, University of Otago, New Zealand; J. Mead, C. Potter, D. Allen, and J. Ososky of the Smithsonian Institution; S. Chivers and K. Danil of the Southwest Fisheries Science Center, La Jolla, California; Marine Mammal Stranding Center, Brigantine, New Jersey; Mystic Aquarium, Mystic, Connecticut; Riverhead Aquarium and Research Foundation, Riverhead, New York; Virginia Aquarium and Marine Science Center, Virginia Beach, Virginia. We also thank the Department of Radiology at The Mount Sinai Hospital, NY, for assistance with CT scans of whale flippers. We give special thanks to the Army Corps of Engineers, Point Caven Facility, Port Liberty, New Jersey, for salvaging many of the listed whale carcasses from New York and New Jersey waters, allowing us to use their drydock facility for necropsies, expert assistance of their ships, cranes, and other heavy machinery during dissections, and arranging prompt disposal of carcasses. We also thank the U.S. Coast Guard for assistance with locating and retrieving several dead whale carcasses at sea. Additional thanks to T. Hieronymus, P. Adam, and J. Geisler for discussions. Funding for this project came from the Lerner

Gray Grant to L.N.C., a travel grant from R.L. Brownell to L.N.C., the San Diego State University Biology Department Student Travel Grant to L.N.C., an NSF grant to A.B., and a NOAA Prescott Marine Mammal Stranding Grant NA03NMF4390402 to J.S.R. This research was completed in partial fulfillment of a Masters of Science degree to L.N.C. in the Department of Biology, San Diego State University.

LITERATURE CITED

- Aguilar A. 2002. F in whale *Balaenoptera physalus*. In: Perrin WF, Würsig B, Thewissen JGM, editors. Encyclopedia of marine mammals. San Diego: Academic Press. p 435–442.
- Albert TF. 1981. Appendix VI: observations on the radiographic anatomy of the pectoral limb of the bowhead whale. In: Albert TF, editor. Tissue structure and functional studies and other investigations on the biology of endangered whales in the Beaufort Sea. Vol II. Final report to the Bureau of Land Management from the Department of Veterinary Science, University of Maryland. NTIS No. PB86-153582/AS. p 917–935.
- Allen GM. 1923. The black finless porpoise, *Meomeris*. Bull Mus Comp Zool 65:233–256.
- Archer CW, Dowthwaite GP, Francis-West P. 2003. Development of synovial joints. Birth Defects Research (Part C) 69:144–155.
- Arnold P, Marsh H, Heinsohn G. 1987. The occurrence of two forms of minke whales in east Australian waters with a description of external characters and skeleton of the diminutive or dwarf form. Sci Rep Whales Res Inst, Tokyo 380:1–46.
- Barnes L, MacLeod SA. 1984. The fossil record and phyletic relationships of Gray whales. In: Jones ML, Schwartz SL, Leatherwood S, editors. The gray whale. San Diego: Academic Press. p 3–32.
- Benke H. 1993. Investigations on the osteology and the functional morphology of the flipper of whales and dolphins (Cetacea). Invest Cetacea 24:9–252.
- Burfield ST. 1920. Note on the hand skeleton of some cetacean fetuses. Proc Trans Liverpool Biol Soc 34:93–96.
- Caldwell MW. 1997. Limb ossification patterns of the ichthyosaur *Stenopterygius*, and a discussion of the proximal tarsal row of ichthyosaurs and other neodiapsid reptiles. Zool J Linn Soc 120:1–25.
- Caldwell MW. 2002. From fins to limbs to fins: limb evolution in fossil marine reptiles. Am J Med Gen 112:236–249.
- Calzada N, Aguilar A. 1996. Flipper development in the Mediterranean Striped Dolphin (*Stenella coeruleoalba*). Anat Rec 245:708–714.
- Carroll RL. 1988. Vertebrate paleontology and evolution. New York: W.H. Freeman and Co. p 698.
- Clack JA. 2002. Gaining ground: the origin and evolution of tetrapods. Indiana: University Press. 369 p.
- Clifford A. 2005. Major transitions in terrestrial artiodactyl forelimbs. J Vertebrate Paleontol 25(Suppl 3):46A.
- Cooper LN, Dawson SD, Reidenberg J, Berta AB. Neuromuscular anatomy and evolution of the cetacean forelimb. Anat Rec (in review).
- Crumly CR, Sanchez-Villagra MR. 2004. Patterns of variation in the phalangeal formulae of land tortoises (Testudinae): developmental constraint, size, and phylogenetic history. Mol Dev Evol 302B:134–146.
- Dawson SD. 2003. Patterns of ossification in the manus of the Harbor Porpoise (*Phocoena phocoena*): hyperphalangy and delta-shaped bones. J Morphol 258:200–206.
- Donoghue M. 1994. Homology. In: Keller EF, Lloyd EA, editors. Keywords in evolutionary biology. Cambridge: Harvard University Press. p 170–179.
- Dooley AC Jr, Fraser NC, Luo ZX. 2004. The earliest known member of the orqual-gray whale clade (Mammalia, Cetacea). J Vertebrate Paleontol 24:453–463.
- Eales NB. 1954. The manus of the Narwhal, *Monodon monoceros* L. Proc R Soc Lond 124:201–211.

- Eschricht DF, Reinhardt J. 1866. On the Greenland right-whale (*Balaena mysticetus*, Linn.) with especial reference to its geographical distribution and migrations in times past and present, and to its external and internal characteristics. In: Flower EH, editor. Recent memoirs on the Cetacea. London: The Ray Society. 150 p.
- Fedak TJ, Hall BK. 2004. Perspectives on hyperphalangy: patterns and processes. *J Anat* 204:151–163.
- Felsenstein J. 1985. Phylogenies and the comparative method. *Am Nat* 125:1–15.
- Fish FE, Rohr JJ. 1999. Review of dolphin hydrodynamics and swimming performance. Technical Report 1801 United States Navy. San Diego: SPAWAR Systems. 131 p.
- Fitzgerald GD. 1970. Comparative morphology of the forelimb skeleton in some Odontoceti (Mammalia, Cetacea). Master of Arts Thesis, Department of Biology, California State College at Long Beach, CA. 138 p.
- Flower WH. 1868. On the osteology of the cachalot or sperm-whale (*Physeter macrocephalus*). *Trans Zool Soc Lond* 6:309–372.
- Flower WH. 1872. On the recent Ziphoid whales, with a description of the skeleton of *Berardius arnouxii*. *Trans R Soc Lond* 8:203–234.
- Flower WH. 1885. Introduction to the osteology of Mammalia. 3rd ed. London: MacMillan and Co. 382 p.
- Gahr M, Kraus C, Pilleri G. 1982. The manus of *Pseudorca crassidens* (Owen): a study of variability. *Invest Cetacea* 13:101–124.
- Gingerich PD, ul Haq M, Zalmout IS, Khan IH, Malkani MS. 2001. Origin of whales from early artiodactyls: hands and feet of Eocene Protocetidae from Pakistan. *Science* 293:2239–2242.
- Goldbogen JA, Calambokidis J, Shadwick RE, Oleson EM, McDonald MA, Hildebrand JA. 2006. Kinematics of foraging dives and lunge-feeding in fin whales. *J Exp Biol* 209:1231–1244.
- Grassé PP. 1967. Traite de zoologie: anatomie, systematique, biologie. Tome XVI, Mammiferes Teguments et Squelette. Vol. XVI, Fascicule I. Paris: Masson et Cie Editeurs, Libraries de Le'Academie de Medecine. 2300 p.
- Howell AB. 1930. Aquatic mammals: their adaptations to life in the water. Springfield: Charles C. Thomas. 338 p.
- International Committee Veterinary Gross Anatomical Nomenclature. 2005. Nomina Anatomica Veterinaria. 5th ed. Gent: World Association of Anatomists.
- Kato H. 2002. Bryde's whales (*Balaenoptera edeni* and *B. brydei*). In: Perrin WF, Würsig B, Thewissen JGM, editors. Encyclopedia of marine mammals. San Diego: Academic Press. p 171–177.
- Kükenthal W. 1889. Die Hand der Cetaceen. *Denkschr D Med Naturwiss Gesell Jena* 3:23–69.
- Kükenthal W. 1893. Vergleichend-anatomische und entwicklungsgeschichtliche untersuchung an waltieren. *Denkschrift der medizinisch-naturwissenschaftlichen gesellschaft zu jena, dritter band* 3:1–447.
- Kunze A. 1912. Über die Brustflosse der Wale. *Zoologische Jahrbücher. Abteilung für Anatomie und Ontogenie der Tiere* 32:577–645.
- Lee KE. 1978. Radiographic anatomy and development of the cetacean flipper. Doctor of Medicine Thesis, Yale University School of Medicine. 37 p.
- Maddison DR, Maddison WP. 2000. MacClade. Version 4. Sunderland: Sinauer Associates. 398 p.
- Martins EP. 2004. COMPARE, version 4.5. Computer programs for the statistical analysis of comparative data. Department of Biology, Indiana University, Bloomington, IN. Distributed by the author at <http://compare.bio.indiana.edu/>.
- Menezes ME, Simões-Lopes PC. 1996. Flipper osteology and morphology of the marine form of *Sotalia fluviatilis* (Cetacea-Delphinidae) in the southern Brazilian coast. Osteologia e morfologia da aleta peitoral da forma marinha de *Sotalia fluviatilis* (Cetacea-Delphinidae) no litoral sul do Brasil. *Estudos de Biologia (Curitiba)* 40:23–31.
- Messenger SL, McGuire JA. 1998. Morphology, molecules and the phylogenetics of cetaceans. *Syst Biol* 47:90–124.
- Motani R. 1999. On the evolution and homologies of Ichthyopterygian forelimbs. *J Vertebrate Paleontol* 19:28–41.
- Muizon C de, McDonald HG, Salas R, Urbina M. 2003. A new early species of the aquatic sloth *Thalassocnus* (Mammalia, Xenarthra) from the Late Miocene of Peru. *J Vertebrate Paleontol* 23:886–894.
- Nikaido M, Hamilton H, Makino H, Sasaki T, Takahashi K, Goto M, Kanda N, Pastene LA, Okada N. 2006. Proceedings of the SMBE Tri-National Young Investigators' Workshop 2005. Baleen whale phylogeny and a past extensive radiation event revealed by SINE insertion analysis. *Mol Biol Evol* 23:866–873.
- O'Keefe FR. 2001. Ecomorphology of plesiosaur flipper geometry. *J Evol Biol* 14:987–991.
- Omura H, Kasuya T. 1976. Additional information on skeleton of the minke whale from the Antarctic. *Sci Rep Whales Res Inst, Tokyo*. 28:57–68.
- Omura H, Ohsumi S, Nemoto T, Nasu K, Kasuya T. 1969. Black right whales in the North Pacific. *Sci Rep Whales Res Inst, Tokyo* 21:1–69.
- Omura H, Ichihara T, Kasuya T. 1970. Osteology of the pygmy blue whale with additional information on external and other characteristics. *Sci Rep Whales Res Inst, Tokyo* 22:1–27.
- Omura H, Kasuya T, Kato H, Wada S. 1981. Osteological study of the Bryde's whale from the central south Pacific and eastern Indian Ocean. *Sci Rep Whales Res Inst, Tokyo* 33:1–26.
- Ortega-Ortiz JB, Villa-Ramirez B, Gersenowies JR. 2000. Polydactyly and other features of the manus of the Vaquita, *Phocoena sinus*. *Mar Mammal Sci* 16:277–286.
- Paterson PA, Janetzki HA, Williams SC. 1997. Osteology of immature dark shoulder minke whales *Balaenoptera acutorostrata* from southern Queensland. *Mem Queensland Mus* 42: 315–325.
- Pilleri G. 1989. *Balaenoptera siberi*, ein neuer spatmiozäner bartenwal aus der Pisco-Formation Perus. In: Pilleri G, editor. Beiträge zur paläontologie der cetaceen Perus. Waldau-Berne, Switzerland: Hirnanatomisches Istitut der Universitat Ostermündigen (Bern). p 65–84.
- Pilleri G. 1990. Paratypus von *Balaenoptera siberi* (Cetacea: Mysticeti) aus der Pisco Formation Perus. In: Pilleri G, editor. Beiträge zur paläontologie der cetaceen und pinnipedier der Pisco Formation Perus II. Waldau-Berne, Switzerland: Hirnanatomisches Istitut der Universitat Bern Ostermündigen (Schweiz). p 205–215.
- Pilleri G, Gahr M. 1976a. The function and osteology of the manus of *Platanista gangetica* and *Platanista indi*. *Invest Cetacea* 7:109–118.
- Pilleri G, Gahr M. 1976b. On the manus of the La Plata Dolphin, *Pontoporia blainvillei*. *Invest Cetacea* 7:119–128.
- Pilleri G, Gahr M. 1976c. The manus of the Amazon Dolphin, *Inia geoffrensis* (de Blainville, 1817) and remarks concerning so called 'polydactyly.' *Invest Cetacea* 7:129–137.
- Rice WR. 1988. Analyzing tables of statistical tests. *Evolution* 43:223–225.
- Richardson MK, Chipman AD. 2003. Developmental constraints in a comparative framework: a test case using variations in phalanx number during amniote evolution. *J Exp Zool (Mol Dev Evol)* 296B:8–22.
- Richardson MK, Oelschläger HA. 2002. Time, pattern, and heterochrony: a study of hyperphalangy in the dolphin embryo flipper. *Evol Dev* 4:435–444.
- Rommel SR. 1990. Osteology of the bottlenose dolphin. In: Leatherwood S, Reeves RR, editors. The bottlenose dolphin. Bar Harbor: Academic Press. p 29–49.
- Rychel AL, Reeder TL, Berta A. 2004. Phylogeny of mysticete whales based on mitochondrial and nuclear data. *Mol Phylogenet Evol* 32:892–901.
- Sanz-Ezquerro JJ, Tickle C. 2003. Digital development and morphogenesis. *J Anat* 202:51–58.
- Sasaki T, Nikaido M, Hamilton H, Goto M, Kato H, Kanda N, Pastene LA, Cao Y, Fordyce RE, Hasegawa M, Okada N. 2005. Mitochondrial phylogenetics and evolution of mysticete whales. *Syst Biol* 56:77–90.
- Schulte H von W. 1916. Anatomy of a fetus *Balaenoptera borealis*. *Mem Am Mus Nat Hist* 1:389–502.
- Sedmera D, Misk I, Klima M. 1997. On the development of cetacean extremities: II. Morphogenesis and histogenesis of the flippers in the spotted dolphin (*Stenella attenuata*). *Eur J Morphol* 35:117–123.
- Shapiro MD, Hanken J, Rosenthal N. 2003. Developmental basis of evolutionary digit loss in the Australian lizard *Hemiergis*. *Mol Dev Evol* 297B:48–56.

- Shubin NH, Alberch PA. 1986. A morphogenetic approach to the origin and basic organization of the tetrapod limb. In: Hecht MK, Wallace B, Prance GT, editors. *Evolutionary biology*. Vol. 20. New York: Plenum Press. p 319–387.
- Stehlin HG von. 1929. Artiodactylen mit fünffingriger Vorderextremität aus dem europäischen Oligocän. *Verhandlungen der Naturforschende Gesellschaft in Basel* 40:599–625.
- Struthers J. 1889. Memoir on the anatomy of the humpback whale. *J Anat Physiol* 1–189.
- Thewissen JGM, Madar SI, Hussain ST. 1996. *Ambulocetus natans*, an Eocene cetacean (Mammalia) from Pakistan. *Courier Forschungsinstitut Senckenberg* 191:1–86.
- Turner W. 1885. The anatomy of a second specimen of Sowerby's whale (*Mesoplodon bidens*) from Shetland. *J Anat* 144–188.
- Turner W. 1892. The lesser roqual *Balaenoptera rostrata* in the Scottish seas, with observations on its anatomy. *Proc R Soc Edinb* 36–75.
- Turner W. 1908. The skeleton of a Sowerby's whale, *Mesoplodon bidens*, stranded at St. Andrews and the morphology of the manus in *Mesoplodon*, *Hyperoodon*, and the Delphinidae. *Proc R Soc Edinb* XXIX VII:387–720.
- Uhen MD. 2004. Form, function, and anatomy of *Dorudon atrox* (Mammalia, Cetacea): an archaeocete from the middle to late Eocene of Egypt. *University of Michigan, Paper on Paleontology* 34:1–222.
- van Beneden PJ, Gervais P. 1880. *Ostéographies des Cétacés Vivants et Fossiles*. Paris: Arthus Bertrand. 634 p.
- Vaughan TA, Ryan JM, Czaplewski NJ. 2000. *Mammalogy*. 4th ed. Toronto: Thomson Learning, Inc. 565 p.
- Watson AG, Bonde RK. 1986. Congenital malformations of the flipper in three west Indian manatees, *Trichechus manatus*, and a proposed mechanism for development of ectrodactyly and cleft hand in mammals. *Clin Orthop Relat Res* 202:294–301.
- Watson AG, Stein LE, Marshall C. 1994. Polydactyly in a bottlenose dolphin, *Tursiops truncatus*. *Mar Mammal Sci* 10:93–100.
- Weber M. 1928. Anatomisches über Cetaceen. Über den Carpus der Cetaceen. *Gegenbaurs Morphologisches Jahrbuch* 13:616–653; plates 27–28.
- Wilkinson M. 1992. Ordered versus unordered characters. *Cladistics* 8:375–385.
- Yablokov AV. 1974. *Variability of mammals*. New Delhi: Amerind Publishing Co. Pvt. Ltd. 350 p.

APPENDIX

TABLE Radiographs examined at the Smithsonian Institution (USNM) and the Los Angeles County Museum (LACM)

	Institution and specimen
Odontocete taxa	
<i>Cephalorhynchus commersonii</i>	USNM 484889, 550156
<i>Cephalorhynchus hectori</i>	USNM 500864
<i>Cephalorhynchus heavisidii</i>	USNM 550067
<i>Delphinapterus leucas</i>	USNM 571021, 504339
<i>Delphinus delphis</i>	USNM 571404, 571410, 550775, 550777, 550779, 550781, 550806, 550808, 550809, 550810, 550811, 550813, 550815, 550861, 550864, 550870, 550872, 550875, 550920, 550921, 550923, 571206, 571208, 571209, 571211, 571212, 571215, 571232, 571234, 571320, 571334, 571397, 571398, 571399, 571400, 571403, 500256, 571233, 571235, 571333, 571396, 571392, 571401, MH85-423, 500261, 500263, 500266, 500272, 504285, 500264, 500270, 500274, 500356, 504219, 504221, 504877, 550041, 550207, 550749, 504406, 504839, 504878, 550206, 550450, 550755, 550470, 550750
<i>Feresa attenuata</i>	USNM 550389
<i>Grampus griseus</i>	USNM 504328, 550108, 550383, 550392, 571350, 504852
<i>Globicephal macrorhynchus</i>	USNM 500224, 504395, 550310, 550424
<i>Globicephal m. meleana</i>	USNM 504593, 504727, 550773
<i>Kogia breviceps</i>	USNM 550361, 550128, 550350, 571228, 504318, 504319, 550477, 550856, 550859, 571324, 571373, 571375
<i>Kogia sima</i>	USNM 504132, 504221, 484981, 550471, 550482, 504594, 571200
<i>Lagenodelphis hosei</i>	USNM 396079
<i>Lagenorhynchus acutus</i>	USNM 571342, 484914, 484915, 484917, 484922, 504148, 504154, 504157, 504160, 484916, 484918, 484923, 504152, 504155, 504158, 504161, 484920, 484925, 504153, 504156, 504159, 504162, 504164, 504166, 504170, 504174, 504182, 571346, 571389, 571395, 504167, 504172, 504179, 571390, 571405, 504165, 504169, 504173, 504180, 571343, 571387, 571393, 571412
<i>Lagenorhynchus albirostris</i>	USNM 550208
<i>Lagenorhynchus obliquidens</i>	USNM 504413, 504415, 504851, 571323
<i>Lissodelphis borealis</i>	550027, 550026, 484929, 571322, 550071
<i>Mesoplodon densirostris</i>	USNM 571325, 486173
<i>Mesoplodon europaeus</i>	USNM 550018, 504610, 550404, 550451, 550824, 571377, 550069, 550362, 504256
<i>Mesoplodon hectori</i>	USNM 504853, JRH052(SWFC0080)
<i>Mesoplodon mirus</i>	USNM ChM A and B, 504612, 504724
<i>Mesoplodon stejnegeri</i>	USNM 504330, 550113
<i>Monodon monoceros</i>	LACM DRP 2254
<i>Phocoena phocoena</i>	USNM 504300, 504301, 504579, 550042, 571458, 571716, 571721, 504304, 504302, 504577, 550312, 571386, 571715, 571724
<i>Phocoena spinipinnis</i>	USNM 550241
<i>Phocoenoides dalli</i>	USNM 504417
<i>Physeter macrocephalus</i>	USNM 550491, 550338, 487416
<i>Pontoporia blainvilliei</i>	USNM 501144, 501169, 501179, 501148, 501172, 501179, 501183, 501147, 501180, 501186
<i>Stenella attenuata</i>	USNM 504025, COA 1, 550016, 550017, 550356, 504274, 550353
<i>Stenella clymene</i>	USNM 550506, 550507, 550509, 550510, 550516, 550508, 550511, 550550

TABLE Radiographs examined at the Smithsonian Institution (USNM) and the Los Angeles County Museum (LACM) (Continued)

	Institution and specimen
<i>Stenella coeruleoalba</i>	USNM 500837, 500836, 500838, 500842, 500852, 504350, 504760, 550043, 550357, 500841, 500848, 504317, 504385, 504859, 550063, 550443, 550495, 571014, 571345, 571363, 571256, 571359
<i>Stenella frontalis</i>	USNM 504321, 550376, 504736, 550748, 571012
<i>Stenella longirostris</i>	504140, 484987, 500859, 504140, 504470
<i>Stenella plagiodon</i>	USNM 550024, 550355, 550102
<i>Steno bredanensis</i>	USNM 550179, 550180, 550217, 55020, 550837, 550368, 504461, 504468, 504469, 504498, 550182, 550218, 55021, 504462, 504494, 504499
<i>Tursiops truncatus</i>	MMS 94018, 941016, 571175, 571254, 571265, 571344, 571370, 571713, 571393, 571119, 571149, 571096, 571065, 571019, 571133, 571150, 571204, 571259, 571269, 571351, 571371, 571121, 571118, 571109, 571094, 571127, 571128, 571134, 571152, 941016, 571253, 571317, 571364, 571372, 571414, 571136, 571093, 571101, 571077, 571030, 571153, 571147, 571154, 571173, 571161, 571167, 571172, 571195, 504123, 504121, 484931, NZP-X3080, 504310, 504501, 504881, 550313, 550440, 571162, 571177, 571193, 571199, 504122, 500857, 504273, 504418, 504541, 550109, 550363, 504295, 504500, 504836, 550309, 550364
<i>Ziphius cavirostris</i>	USNM 550405, 550734, 504327, 504094
Mysticete taxa	
<i>Balaena mysticetus</i>	LACM 54477, 72159, 72484
<i>Balaenoptera acutorostrata</i>	LACM 54808
<i>Balaenoptera musculus</i>	USNM-Santa Cruz radiograph
<i>Balaenoptera physalus</i>	USNM 550116
<i>Eschrichtius robustus</i>	LACM 54543, 54544, 54547, 54549, FED 4480